G. Gyarmati, D. Molnár
Inštitut za kemijsko metalurgijo in livarstvo, Univerza v Miskolcu (HU) /
Institute of Chemical Metallurgy and Foundry Engineering, University of Miskolc (HU)

Analiza kakovosti ingotov iz različnih aluminijevih zlitin

Analysis of the quality of different aluminum alloy ingots

Povzetek

Pretekle raziskave so pokazale, da se lahko kakovost ingotov, ki jih proizvedejo različni dobavitelji primarnih ali sekundarnih zlitin, bistveno razlikuje. Tako lahko vsebnost nečistoč v ingotih, ki se uporabljajo kot vložek, vpliva na kakovost tekoče kovine in ulitkov iz nje. V tem delu je bila uporabljena spremenjena tehnika preskusa z zmanjšanim tlakom (RPT), ki temelji na pretaljevanju vzorcev, pridobljenih iz ingotov, za ugotavljanje kakovosti primarnih ingotov iz zlitine AlSi9Mn, izdelanih s tehnikama horizontalnega polkontinuiranega litja (HDC) in gravitacijskega litja. Za ocenjevanje kakovosti kovine je bila opravljena analiza slik prečnih prerezov. Določeni so bili delež površine s porami, številčna gostota, normaliziran indeks bifilma in normaliziran skupni obseg por ter analizirana razmerja med različnimi metrikami. Opravljena je bila primerjava rezultatov z oceno kakovosti taline staljenih serij, izdelanih iz ingotov. Izvedene so bile simulacije strjevanja, termična analiza in mikrostrukturne preiskave, da bi ugotovili pogoje strjevanja tradicionalnih in pretaljenih vzorcev za preskus z zmanjšanim tlakom. Na podlagi rezultatov je razvidno, da imajo ingoti, uliti s tehniko horizontalnega polkontinuiranega litja, nižje koncentracije oksidov in plinov, kar je mogoče pripisati razlikam v tehnikah priprave taline in ulivanja ingotov. Primerjava parametrov, ocenjenih z analizo slik, je pokazala, da obstaja močna linearna povezava med normaliziranim indeksom bifilma in normaliziranim skupnim obsegom por. Izpostavljeni so možni viri napak pri ocenjevanju kakovosti ingotov.

Ključne besede: aluminijeva zlitina, ingot; kakovost kovine; preskus z zmanjšanim tlakom, bifilm, litje

Abstract

Previous research has revealed that the quality of ingots produced by different primary or secondary alloy suppliers can differ significantly. In this way, the quality of the liquid metal and the castings made from it can be affected by the impurity content of the ingots used as charge material. In this work, a modified reduced pressure test (RPT) technique, which is based on the remelting of samples extracted from ingots, was applied to investigate the quality of primary AlSi9Mn ingots made by horizontal direct-chill (HDC) casting and gravity casting techniques. For the evaluation of metal quality, image analysis of the cross-sections was applied. Pore area fraction, number density, normalized Bifilm-Index, and normalized total pore perimeter were determined, and the relationships between the different metrics were analyzed. The results were compared with the melt quality assessment of the as-melted batches made from the ingots. Solidification simulations, thermal analysis, and microstructural investigations were conducted to investigate the solidification conditions of traditional and remelted RPT samples. Based on the results, the HDC cast ingots possess lower oxide and gas concentrations, which can be traced back to the differences in the

melt preparation and casting technologies of the ingots. The comparison of the parameters evaluated by image analysis revealed that there is a strong linear relationship between the normalized Bifilm-Index and the normalized total pore perimeter. The possible sources of error in ingot quality evaluation are highlighted.

Keywords: aluminum alloy; ingot; metal quality; reduced pressure test; bifilm; casting

1 Uvod

Ne glede na tehnologijo litja, ki se uporablja za izdelavo ulitih sestavnih delov, igra kakovost taline bistveno vlogo pri zagotavljanju visoke strukturne celovitosti, mehanskih lastnosti in preprečevanju napak pri litju, kot so poroznost, puščanje, pokanje v vročem in razpoke [1–3]. Že prvo od znanih desetih pravil, ki jih je oblikoval *Campbell* [4, 5], da bi določil temeljne zahteve za izdelavo visokokakovostnih kovinskih ulitkov, poudarja, da je pomembno »začeti z dobro kakovostno talino«. Da bi to dosegli, je treba skrbno izbrati, izvesti in nadzorovati korake taljenja, prenosa taline in obdelave taline. Vendar se lahko kakovost ingotov, ki jih proizvedejo različni dobavitelji primarnih ali sekundarnih zlitin, močno razlikuje. Tako na kakovost taline vpliva vsebnost nečistoč v ingotih, ki se uporabljajo kot vložek [6]. Vsi ingoti niso izdelani na enak način: proizvajalci kakovostnih ingotov uporabljajo linijsko razplinjevanje in filtre. Če izbrani dobavitelj ne uporablja ustreznega postopka obdelave taline, morajo livarne spremeniti svoje metode obdelave taline, da bi se izognile povečanju poroznosti in z oksidi povezanega izmeta [7]. Drugo ključno vprašanje je metoda litja ingotov. Če se ingoti ulivajo s turbulentnim litjem, so lahko učinki obdelave taline ovirani [8].

Grandfield [9] je izčrpno pregledal proizvodne metode pretaljevanja ingotov iz aluminija in aluminijevih zlitin. Najpogostejša tehnologija za proizvodnjo ingotov livarskih zlitin je gravitacijsko litje v odprte kokile, ki so navadno nameščena v transportno linijo za ingote **(Slika 1. (a)).** V ta namen se

1 Introduction

Regardless of the casting technology used for manufacturing cast components, liquid metal quality has an essential role in providing high structural integrity, mechanical performance, and the avoidance of casting defects such as porosity, leakage, hot tears, and cracks [1-3]. Even the first of the well-known ten rules, created by *Campbell* [4, 5] to provide the fundamental requirements for the manufacture of high-quality metal castings, emphasizes the importance of “starting with a good-quality melt”. To accomplish this, the melting, melt-transfer, and melt-processing steps need to be carefully selected, executed, and controlled. However, the quality of the ingots produced by different primary or secondary alloy suppliers can differ remarkably. In this way, the melt quality is affected by the impurity content of the ingots used as charge material [6]. Not all ingots are created the same way: quality ingot producers use in-line degassing and filters. If the selected supplier is not using appropriate melt treatment, the foundries need to modify their melt treatment methods to avoid an increase in porosity and oxide-related scrap [7]. Another critical issue is the casting method of the ingots. If the casting of ingots is performed by pouring turbulently, the effects of melt treatments can be hindered [8].

The production methods of remelting aluminum and aluminum alloy ingots were comprehensively reviewed by *Grandfield* [9]. The most common technology to produce foundry alloy ingots is gravity casting into

navadno uporabljajo litoželezne ali jeklene kokile, polnjenje pa poteka z livnim kolesom ali avtomatskimi livnimi ponovcami. Hitrost transportne linije je običajno optimizirana za povečanje produktivnosti, pri čemer je treba upoštevati tudi hitrost strjevanja. Zato so kokile pogosto hlajene z vodo, da se doseže večja hitrost proizvodnje. Na kakovost zlitine in nastajanje oksidov med polnjenjem vplivajo predvsem zasnova livnega kolesa ali ponovce ter postopki ravnanja s talino in obdelave pred litjem. Proizvajalce ingotov zanima predvsem ohranjanje visokih proizvodnih hitrosti, pri čemer je nastajanje oksidov med ulivanjem čim manjše. Številne študije [10–12] kažejo, da je mogoče z optimizacijo faze polnjenja učinkovito zmanjšati nastajanje žlindre in vnašanje oksidov. Vendar pa tudi pri uporabi optimiziranega polnjenja kokile sama metoda ni brez oksidov in zajemanja zraka, zlasti pri običajnih proizvodnih stopnjah, ki se uporabljajo v industriji. Druga pogosta težava gravitacijsko ulitih ingotov je, da imajo običajno luknje zaradi krčenja, ki lahko vsebujejo celo vodo, kar je posledica vodnega hlajenja neposredno na ingotu ali neustreznega skladiščenja [13]. Zaradi tega obstaja nevarnost eksplozij, če se z vodo kontaminirani ingoti polnijo neposredno v talino [14]. Vedno bolj se uveljavlja uporaba linijskega razplinjevanja in filtrov iz keramične pene pred gravitacijskim litjem ingotov, kar bi lahko pripomoglo k zmanjšanju vsebnosti vključkov v kovini [7, 9].

Horizontalno polkontinuirano litje (HDC) je še ena pogosta tehnologija za proizvodnjo livarskih ingotov. HDC je postopek neprekinjenega litja, pri katerem se talina dovaja iz vmesne ponvice do kokil hlajenih z vodo, skozi ognjevarno prenosno cev **(Slika 1. (b)).** Valj za odvzem deluje z zahtevano hitrostjo litja. Palice, ulite s postopkom HDC, imajo strogo nadzorovane

open molds that are typically assembled into an ingot conveyor line (**Figure 1 (a)**). Cast iron or steel molds are generally used for this purpose, and the filling is executed through a casting wheel or automated casting ladles. The speed of the conveyor line is usually optimized to maximize productivity, while the solidification rate also needs to be considered. For this reason, the molds are often water-cooled to achieve higher production rates. In terms of metal quality and dross formation during filling, the design of the casting wheel or ladle, as well as the upstream melt handling and treatment methods, are the main influences. Ingot producers are mainly interested in maintaining high-production rates, while dross formation during pouring is kept at a minimum. There are numerous studies [10-12] that show that by optimizing the filling stage, dross formation and oxide entrainment can be effectively lowered. However, even when optimized mold filling is utilized, the method itself is not free of oxide and air entrainment, especially at the common production rates applied by the industry. Another common problem of gravity-cast ingots is that they usually have shrinkage cavities, which can even contain water as a result of applying water cooling directly on the ingot or as a result of inappropriate storage [13]. This holds the risk of explosions if water-contaminated ingots are charged directly to liquid metal [14]. There has been a growing trend to apply in-line degassing and ceramic foam filters before gravity casting of the ingots, which could help in lowering the inclusion content of the metal [7, 9].

Horizontal direct-chill casting (HDC) is another common technology to produce foundry ingots. HDC is a continuous casting process in which liquid metal is fed from the tundish to water-cooled molds through a refractory transfer tube and an orifice plate

dimenzije in običajno nimajo razpok ali lukenj zaradi krčenja. Ker postopek ne vključuje ulivanja in talina ne pada prosto, je koncentracija žlindre in ujetih oksidov veliko manjša kot pri litju v odprte kokile. Na zahtevanih dolžinah se palice odrežejo z žago za odrezovanje, ki je sinhronizirana z valjem za odvzem [9, 15]. Stroji za litje so običajno povezani s talilnimi pečmi prek sistema za odstranjevanje nečistoč iz kovin, ki vključuje enote za razplinjevanje in filtrske škatle [16, 17].

Pri izbiri dobavitelja materiala za vložek je treba kot pomembno nalogo obravnavati odkrivanje in količinsko določanje nečistoč, prisotnih v ingotih. Literatura za to nalogo navaja različne pristope. Večina teh metod za karakterizacijo temelji na preskusu z zmanjšanim tlakom (RPT). *Fox* in *Campbell* [18, 19] sta poročala, da je preskus RPT lahko učinkovito orodje za ocenjevanje kakovosti taline. Med strjevanjem pod zmanjšanim tlakom se plini, ki se zadržujejo med plastmi napak bifilma, raztezajo [20]. Poleg tega se topnost vodika v zlitini zmanjša zaradi nižjega delnega tlaka (**Figure 1 (b)**). The withdrawal roll is driven at the required casting speed. HDC cast bars have tight dimensional controls and usually no cracks or shrinkage cavities. As the process does not involve any pouring action and there is no free-falling liquid metal, there is much lower dross and entrained oxide concentration than in open mold casting. At the required lengths, the bars are cut with a cut-off saw, which is synchronized with the withdrawal roll [9, 15]. The casting machines are generally connected to the melting furnaces through a metal launder system, which involves inline degassing units and filter boxes [16, 17].

The detection and quantification of impurities present in ingots should be considered as an important task when selecting the supplier of the charge material. There are different approaches available in the literature for this task. Most of these characterization methods are based on the reduced pressure test (RPT). *Fox* and *Campbell* [18, 19] reported that RPT can be an effective tool in the evaluation of liquid

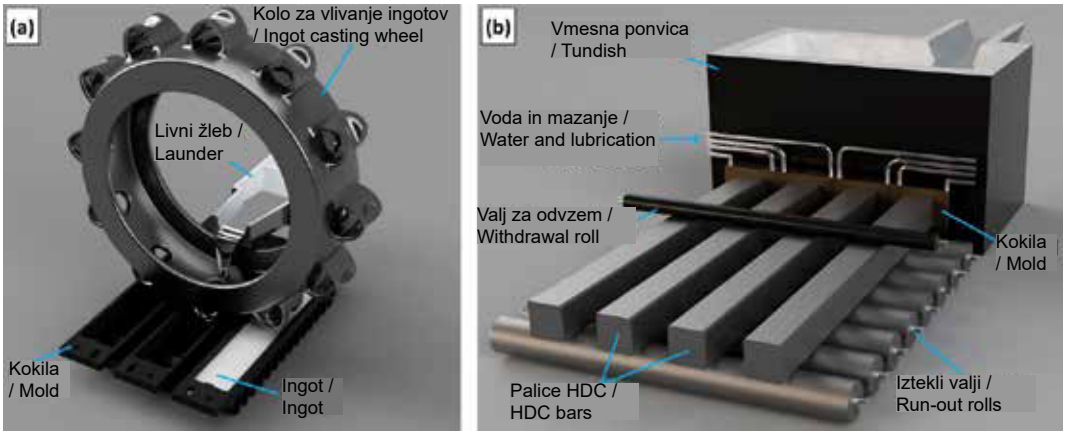

Slika 1. Shematski prikaz (a) gravitacijskega litja (GC) v odprte kokile in (b) horizontalnega polkontinuiranega litja (HDC)

Figure 1. Schematic illustration of (a) gravity casting (GC) into open molds and (b) horizontal direct-chill casting (HDC)

vodika, kar povzroči večje izločanje H_2 [21]. Posledica teh dejavnikov je, da se napake dvojnega oksidnega filma znotraj vzorcev RPT razširijo, kar omogoča lažje odkrivanje z rentgensko radiografijo ali kvantitativno analizo slike na poliranem prerezu [18]. *Dispinar* in *Campbell* [22] sta uvedla tako imenovani indeks bifilma (BI), ki se lahko uporablja za količinsko opredelitev vsebnosti bifilma v talini na podlagi vsote največjih dolžin por, ugotovljenih na prečnem prerezu vzorcev RPT.

Dispinar in *Campbell* [23] sta preučila učinke zmanjšanja višine prostega padanja in turbulence znotraj livnega žleba na kakovost gravitacijsko ulitih sekundarnih livarskih ingotov. Njuna metoda za karakterizacijo je vključevala pretaljevanje ingotov v indukcijski peči in odvzem vzorcev RPT, nato pa sta ocenila gostoto in vrednosti indeksa bilfma. Z zmanjšanjem višine padanja in izboljšanjem pretoka v livnem žlebu z oblikovnimi spremembami, se je jasno izboljšala kakovost zlitin: gostota vzorcev RPT se je povečala, medtem ko se je indeks biflma učinkovito zmanjšal. Vendar so spremembe zmanjšale hitrost proizvodnje, ki je za nekatere dobavitelje ingotov pomembnejši parameter kot kakovost kovine. *Erzi* in drugi [6] so predlagali razmeroma zapleteno metodo za ocenjevanje kakovosti ingotov različnih dobaviteljev. Iz preiskovanih ingotov se pripravijo 10-kilogramske šarže, po taljenju pa se ulijejo vzorci za RPT, livnost in natezni preskus. Tako imenovani dobaviteljev indeks kakovosti se nato izračuna iz indeksa bifilma, dolžine livnosti in nateznih lastnosti. Metoda *Erzija* in *Tiryakioğluja* [24] vključuje izrez vzorca iz sredine preiskovanega ingota in njegovo mehansko obdelavo na točno določeno velikost lončka za vzorčenje RPT. Vzorec se stali v lončku in strdi v delnem vakuumu. Nato se z metalografskimi metodami ali

metal quality. During solidification under reduced pressure, the entrained gases between the layers of bifilm defects are expanded [20]. In addition, the solubility of hydrogen in the alloy is reduced by the lower hydrogen partial pressure, which results in enhanced H_2 precipitation [21]. The consequence of these factors is that double oxide film defects inside the RPT samples are expanded, which allows easier detection by X-ray radiography or quantitative image analysis on a polished section [18]. *Dispinar* and *Campbell* [22] introduced the so-called Bifilm-Index (BI), which can be used to quantify the bifilm content of the molten metal based on the sum of the maximum lengths of pores found on the cross-section of RPT samples.

Dispinar and *Campbell* [23] investigated the effects of reducing the free-falling height and the turbulence inside the casting launder on the quality of gravity-cast secondary foundry ingots. Their characterization method involved the remelting of the ingots in an induction furnace and taking RPT samples, then the density and the Bifilm-Index values were evaluated. There was a clear improvement in the metal quality by reducing the falling height and by improving the flow inside the launder by design modifications: the density of the RPT samples increased while the Bifilm-Index was effectively reduced. However, the production rate was lowered by the modifications, which tends to be a more important parameter for some ingot suppliers than metal quality. *Erzi* et al. [6] proposed a relatively complex method for assessing the quality of ingots from different suppliers. 10 kg charges are prepared from the investigated ingots, and after melting, RPT, spiral fluidity, and tensile test specimens are cast. The so-called Supplier's Quality Index is then calculated from the Bifilm-Index, fluidity length, and

računalniško tomografijo (CT) odkrijejo in količinsko opredelijo pore v vzorcu. *Erzi* in *Tiryakioğlu* sta s primerjavo rezultatov analize slike prečnega prereza vzorcev RPT in analize poroznosti z računalniško tomografijo ugotovila, da obe metodi dajeta podobne rezultate. Podoben pristop sta uporabila tudi *Hsu* in *Li* [25], ki sta pretaljene vzorce RPT uporabila za ugotavljanje vpliva različnih zasnov ulivnih sistemov in filtrov iz keramične pene na kakovost kovine. Njihova metoda je vključevala rezanje majhnih vzorcev (3 × 3 × 7 cm) in taljenje v lončkih za vzorčenje RPT pri 700 °C s časom zadrževanja v peči 1 uro.

Fox in *Campbell* [19] prav tako omenjata, da so bili med razvojem njunih testov pretaljevanja izvedeni začetni poskusi z isto metodo, ki sta jo predlagala *Erzi* in *Tiryakioğlu* [24] (tj. izdelava vzorca v točno določeni velikosti lončka za vzorčenje RPT in pretaljevanje v njej), ki je bila dolgotrajna in lahko povzroči zračne žepe med vzorcem in steno lončka, kar lahko med pretaljevanjem povzroči plinsko poroznost. Zato sta *Fox* in *Campbell* predlagala uporabo poroznega medija, kot je pesek ali aluminijev oksid, ki lahko med pretaljevanjem podpira vzorec v majhnem vsebniku, kot je jeklena posodica. Po našem vedenju ta metoda še ni bila uporabljena v nobenem objavljenem raziskovalnem delu, njeni podrobni tehnični parametri, ki omogočajo ustrezno preučitev kakovosti kovine, pa v literaturi niso pojasnjeni. Po navedbah omenjenih avtorjev je mogoče pri tej metodi uporabiti katero koli geometrijo vzorca. Vendar bi bilo praktično uporabiti geometrijo vzorca, temperaturo pretaljevanja in količino poroznega medija, ki omogočajo podobno hitrost strjevanja kot pri tradicionalnih vzorcih RPT. Hitrost strjevanja je ključni dejavnik pri nastajanju poroznosti [26–28]. Prevelika hitrost strjevanja lahko ovira rast por, medtem ko lahko prepočasno strjevanje

tensile properties. The method of *Erzi* and *Tiryakioğlu* [24] involves cutting out a sample from the middle of the investigated ingot and machining it to the exact size of the RPT sampling cup. The specimen is melted inside the cup and solidified in a partial vacuum. Then, the detection and quantification of pores in the sample are conducted with either metallographic methods or computed tomography (CT). By comparing the results of the image analysis of the cross-section of the RPT samples and the CT porosity analysis, *Erzi* and *Tiryakioğlu* concluded that both methods yield similar results. A similar approach was utilized by *Hsu* and *Li* [25], who used remelted RPT samples for the characterization of the effect of different gating system designs and ceramic foam filters on the metal quality. Their method involved sectioning small samples (3x3x7 cm) and remelting them in the RPT sampling cups at 700 °C with a furnace residence time of 1 hour.

Fox and *Campbell* [19] also mention that during the development of their remelting tests, initial trials were carried out with the same method suggested by *Erzi* and *Tiryakioğlu* [24] (i.e., machining a sample to the exact size of the RPT sampling cup and remelting in it), which were time-consuming and can result in air pockets being trapped between the sample and the crucible wall, which can cause air-entrainment during remelting. For this reason, *Fox* and *Campbell* suggested the use of a porous medium such as sand or alumina that can support the specimen in a small container, like a steel cup, during remelting. To the best of our knowledge, this method has not been adopted by any published research work yet, and its detailed technical parameters that allow proper investigation of metal quality are not clarified in the literature. According

v delnem vakuumu povzroči odstranjevanje plina v obliki mehurčkov, ki počijo na površini (podobno kot pri vakuumskem razplinjevanju) [29]. Zato je bil namen pričujočega raziskovalnega dela preizkusiti metodo *Foxa* in *Campbella* za opredelitev kakovosti ingotov iz aluminijevih zlitin in raziskati pogoje strjevanja med uporabo te metode. V ta namen so bile izvedene simulacije strjevanja, izbrani parametri pa so bili preizkušeni s preiskavo kakovosti ingotov iz primarne aluminijeve zlitine, proizvedenih z različnimi tehnologijami. Opravljena je bila primerjava rezultatov z oceno kakovosti taline staljenih serij, izdelanih iz ingotov.

3 Materiali in preskusni postopek

Predlagani postopek pretaljevanja je shematično prikazan na **Sliki 2.** Majhni vzorci so izdelani iz ingotov preiskovane zlitine in staljeni v kremenčevem pesku pri 700 °C. Kot talilni medij smo uporabili nevezan kremenčev pesek s povprečno velikostjo zrn 0,35 mm. Za te preizkuse je bil izbran vzorec velikosti 20 × 20 × 10 mm, ki se je zlahka prilegel v posodico za vzorec RPT. Po taljenju se vzorec prenese v vakuumsko komoro naprave RPT. Po strjevanju je mogoče vzorce preučiti z računalniško tomografijo ali z analizo slik prečnih prerezov, narejenih po ustrezni metalografski pripravi. V tem delu je bil izbran slednji pristop.

Izbira sipkega peska kot talilnega medija je temeljila na delu *Foxa* in *Campbella* [19], ki sta poročala, da se pri pretaljevanju vzorcev (ki so obdelani na natančno velikost jeklenih posodic) v jeklenih posodicah lahko med vzorcem in steno lončka ujamejo zračni žepi, kar lahko med pretaljevanjem povzroči zajetje zraka. Ker ima sipek pesek visoko prepustnost

to the mentioned authors, any sample geometry can be used for this method. However, it would be practical to use a sample geometry, remelting temperature, and porous medium quantity that allows a similar solidification rate as in the case of traditional RPT samples. The solidification rate is a critical factor in porosity formation [26-28]. Too high solidification speed can hinder pore growth, while too slow solidification under partial vacuum can result in gas removal in the form of bubble bursting on the surface (similarly to vacuum degassing) [29]. Consequently, the present research work aimed to test the method of *Fox* and *Campbell* for the characterization of the quality of aluminum alloy ingots and to investigate the solidification conditions during the utilization of the method. For this, solidification simulations were conducted, and the selected parameters were tested by investigating the quality of primary aluminum alloy ingots produced by different technologies. The results were compared with the melt quality assessment of as-melted batches made from the ingots.

3 Materials and Experimental Procedure

The proposed remelting procedure is schematically illustrated in **Figure 2**. Small samples are machined from the investigated alloy ingots and melted in silica sand at 700 °C. We used unbonded loose silica sand as a melting medium with an average grain size of 0.35 mm. For these tests 20 × 20 × 10 mm sample size was selected, which fit easily into the RPT sample cup. After melting, the sample is taken to the vacuum chamber of the RPT apparatus. Following solidification, the specimens can be investigated by computed tomography or by the image analysis of cross-

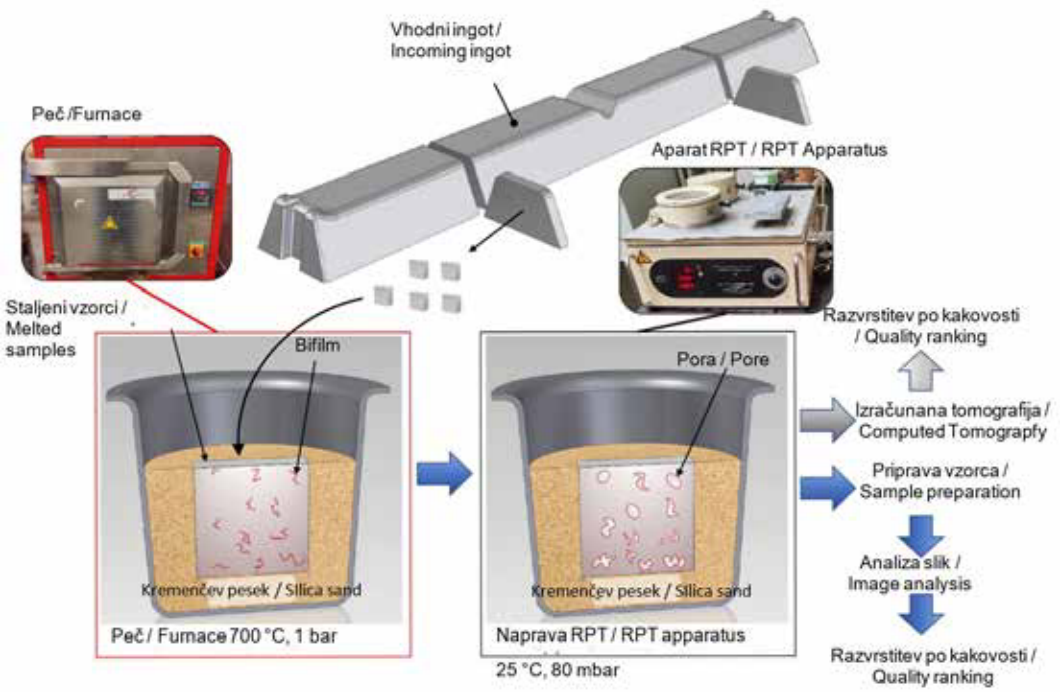

Slika 2. Shema ocenjevanja kakovosti materiala ingota

Figure 2. The scheme for the quality assessment of the ingot material

za pline, zrak med zrni peska, ki obdajajo vzorec kovine, ne more vstopiti v vzorec kovine, saj bi za vstop v tekočo kovino skozi površinsko oksidno plast potreboval večji tlak kot za izstop skozi pore med zrni peska.

V prvem koraku naše preiskave smo izvedli simulacije strjevanja s pomočjo modula za gravitacijsko litje programske opreme za simulacijo NovaFlow&Solid, da bi raziskali razlike med hitrostjo strjevanja tradicionalnih in pretaljenih vzorcev RPT. Najprej je bilo simulirano strjevanje tradicionalnega vzorca RPT **(Slika 3. (a)),** ulitega iz Al-9,5%Si-0,4%Mn-0,15% Fe (teža 90 g), pri temperaturi ulivanja 700 °C. Za orodje je bila izbrana jeklena čaša (s toplotno prevodnostjo 26 W/m·K), segreta na 300 °C, z 0,8 mm debelo ognjevzdržno prevleko (s toplotno

sectional images made after appropriate metallographic preparation. The latter approach was chosen in this work.

The selection of loose sand as a melting medium was based on the work by *Fox* and *Campbell* [19], who reported that remelting samples (which are machined to the exact size of the steel cups) in steel cups can result in air pockets being trapped between the sample and the crucible wall, which can cause air-entrainment during remelting. As loose sand has high gas permeability, the air between the sand grains surrounding the metal sample cannot enter the metal sample, as it would require more pressure to enter the liquid metal through the surface oxide layer than escaping through the pores between the sand grains.

prevodnostjo 0,25 W/m-K). Nato smo simulirali strjevanje pretaljenega vzorca velikosti 20 × 20 × 10 mm s kremenčevim peskom kot materialom orodja (z izbrano toplotno prevodnostjo 0,3 W/m-K [30]) in jekleno čašo RPT kot posodo **(Slika 3. (b, c)).** Začetna temperatura vzorca in orodja je bila 700 °C. Med simulacijami sta bili preizkušeni dve količini peska: 55 g, kar zadostuje za popolno zapolnitev jeklene čaše **(Slika 3. (b)),** in 30 g **(Slika 3. (c)),** kar je bilo izbrano zaradi skrajšanja časa strjevanja. Za poskuse v realnih okoliščinah je bila izbrana količina 30 g peska. Razlog za to izbiro je, da je bilo med predhodnimi preskusi s posodicami za vzorčenje, popolnoma napolnjenimi s peskom, ugotovljeno, da je bila zgornja površina vzorca popolnoma tekoča tudi po 1,5 minute, na vrhu vzorca pa so se pojavili mehurčki plina, kar lahko resno spremeni natančnost ocene kakovosti.

Preiskovani ingoti AlSi9Mn so bili izdelani z dvema različnima tehnologijama: s horizontalnim polkontinuirnim litjem **(Slika 4. (a, b))** in gravitacijskim litjem v odprto kokilo **(Slika 4. (c, d)).** Iz obeh vrst ingotov smo izrezali dve 1 cm debeli rezini, nato pa iz vsake rezine pridobili 5 vzorcev, kot je razvidno iz **Slik 4 (b)** in **(d)** (10 vzorcev za obe vrsti ingotov). Pred taljenjem smo

As the first step of our investigation, we conducted solidification simulations with the aid of the gravity casting module of the NovaFlow&Solid simulation software to investigate the differences between the solidification rates of traditional and remelt RPT samples. First, the solidification of a traditional RPT sample (**Figure 3 (a)**) cast from Al-9.5%Si-0.4%Mn-0.15%Fe (weighing 90 g) was simulated with a casting temperature of 700 °C. The mold was selected to be a steel cup (with a thermal conductivity of 26 W/m·K) preheated to 300 °C with a 0.8 mm thick refractory coating (with a thermal conductivity of 0.25 W/m·K). Then, the solidification of a remelted sample with sizes of 20 × 20 × 10 mm was simulated with silica sand mold material (with a selected thermal conductivity of 0.3 W/m·K [30]) and the RPT steel cup as a container (**Figure 3. (b, c)**). The starting temperature of the sample and the mold was 700 °C. During the simulations, two sand quantities were tested: 55 g, which is enough to fill the steel cup **(Figure 3. (b))**, and 30 g (**Figure 3. (c)**), which was selected in an attempt to decrease solidification time. For real-life experiments, the 30 g sand quantity was chosen. The reason for this choice is that during preliminary tests with sampling cups filled fully with sand, it was discovered

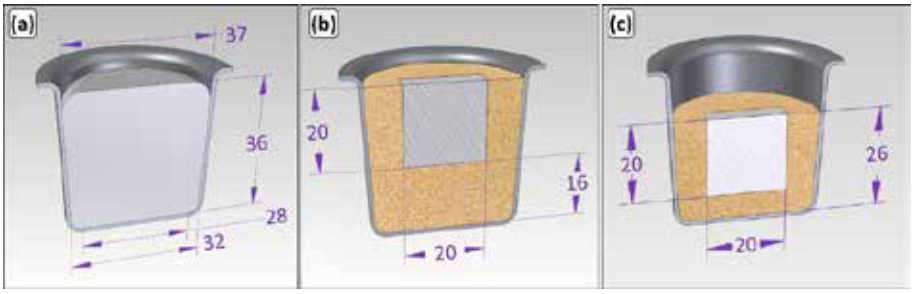

Slika 3. Prečni prerez geometrij, uporabljenih za simulacije strjevanja, (a) vzorec RPT in (b, c) vzorci, pretaljeni v peščeni podlagi

Figure 3. Cross-sectional view of the geometries used for solidification simulations, (a) RPT specimen and (b, c) samples remelted in sand support

vzorce 1 uro hranili pri 500 °C v peči, da bi odstranili morebitne nečistoče in hidrokside, ki so nastali med rezanjem vzorcev. Pred prvo uporabo je bil pesek, ki je bil uporabljen kot talilno sredstvo, predhodno segret in 1 uro vzdrževan pri 700 °C, da se odstranijo morebitne hlapne nečistoče in olajša postopek taljenja vzorcev zlitine. Vzorci zlitine so bili vstavljeni v predhodno segret pesek in 15 minut vzdrževani pri 700 °C. Relativna vlažnost v delavnici je bila med vsemi poskusnimi fazami med 50 % in 60 %.

Na podlagi predhodne toplotne analize je 15 minut dovolj, da se vzorci stalijo in dosežejo temperaturo peska. Vzorci so se strdili v vakuumski komori naprave RPT s tlakom 80 mbar in 6 minutami zadrževanja. Čeprav za utrjevanje peska ni bilo uporabljeno vezivo, so vzorci odlično ohranili obliko **(Slika 5)**

Kot dodaten preizkus so bili tradicionalni vzorci RPT odvzeti iz vzorcev

that the top surface of the specimen was completely liquid even after 1.5 minutes, and gas bubbles were bursting at the top of the sample, which can seriously alter the accuracy of quality evaluation.

The investigated AlSi9Mn ingots were manufactured by two different technologies: horizontal direct-chill casting **(Figure 4 (a, b))** and open mold gravity casting (**Figure 4 (c, d)**). Two, 1 cm thick slices were cut from both types of ingots, then 5 samples were extracted from each slice, as can be seen in **Figure 4 (b)** and **(d)** (10 samples for both ingot types). Before melting, the samples were held at 500 °C for 1 hour in a muffle furnace to remove any possible contaminations and hydroxides formed during the cutting of the samples. Before the first use, the sand being used as a melting medium was preheated and held at 700 °C for 1 hour to remove any possible volatile impurities and to facilitate the melting process of the alloy samples.

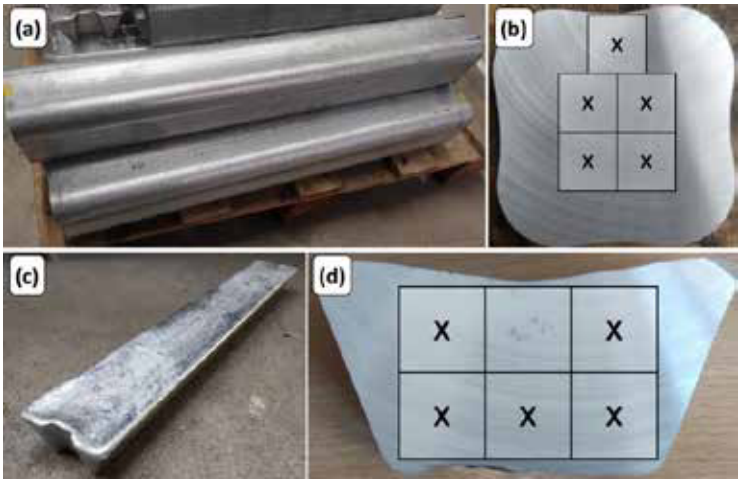

Slika 4. (a, b) Horizontalni polkontinuirano uliti in (c, d) gravitacijsko uliti ingoti, mesta vzorčenja so označena v (b) in (d)

Figure 4. (a, b) Direct-chill cast and (c, d) gravity cast ingots, sampling places are indicated in (b) and (d)

Slika 5. Ohranjanje oblike med pretaljevanjem in strjevanjem pod zmanjšanim tlakom

Figure 5. Shape retention during remelting and solidification under reduced pressure

ingotov (teža 500 g), ki so bili staljeni v glineno-grafitnem lončku pri 700 °C. Takoj po doseganju temperature litja so bili uliti 3 vzorci. Metoda vzorčenja je podrobno opisana v ref. [31]. Kemijska sestava vzorcev ingotov je bila analizirana z optično emisijsko spektroskopijo, ki je pokazala minimalno razliko med obema vrstama ingotov **(Preglednica 1).**

Preglednica 1. Koncentracija legirnih elementov v preučevanih ingotih iz aluminijevih zlitin (masni %)

Table 1. Concentration of the alloying elements of the studied aluminum alloy ingots (wt. %)

Vzorec / Sample	Litje HDC / HDC cast	Gravitacijsko litje / Gravity cast
Si	9,38	8,81
Fe	0,145	0,134
Mn	0,515	0,474
Zn	0,004	0,021
Ti	0,013	0,072
Sr	0,011	0,014
Zr	0,001	0,103
∑ drugo	najv. / max 0,10	najv. / max 0,10

Preskusi termične analize so bili opravljeni na vzorcih s tradicionalno geometrijo RPT in geometrijo pretaljenih vzorcev. Za te preizkuse je bil uporabljen termočlen tipa K s premerom 1 mm, ki je bil zaščiten z ovojem iz nerjavnega jekla. V obeh primerih so bile posodice RPT nameščene na izolacijski ognjevzdržni blok. Preden smo termočlen navpično spustili v pretopljeni vzorec RPT, smo ga s pihalnim gorilnikom segreli na približno 650 °C, da bi preprečili odvajanje odvečne toplote iz majhnega vzorca. Pri tradicionalni geometriji RPT je bila jeklena čaša predhodno segreta na 300 °C. Podatke o temperaturi je zbiral sistem za zbiranje podatkov (National Instruments NI-9211), povezan z osebnim računalnikom, s frekvenco vzorčenja 4 Hz.

The alloy samples were plugged into the preheated sand and were held at 700 °C for 15 minutes. The relative humidity levels in the workshop were between 50 % and 60 % during all experimental steps.

Based on preliminary thermal analysis, 15 minutes is enough for the specimens to melt and reach the temperature of the sand. The samples were solidified in the vacuum chamber of an RPT apparatus with 80 mbar pressure and 6 minutes of residence time. Although no binder was used to cure the sand, the shape retention of the specimens was excellent **(Figure 5).**

As an additional test, traditional RPT samples were taken from ingot samples (weighing 500 g), which were melted in a clay-graphite crucible at 700 °C. 3 samples were cast immediately after reaching the casting temperature. The sampling method is described in detail in ref. [31]. The chemical composition of the ingot samples was analyzed with optical emission spectroscopy, which showed a minimal difference between the two types of ingots **(Table 1)**.

Thermal analysis tests were conducted on samples with the traditional RPT and remelt sample geometries. For these tests, a K-type thermocouple with a 1 mm diameter was used, which was protected by a stainless steel sheath. In both cases, the RPT cups were placed on an insulating refractory block. Before the thermocouple was vertically lowered into the remelted RPT sample, it was preheated to approximately 650 °C with a blow torch, to avoid excess heat extraction from the small-sized sample. In the case of the traditional RPT geometry, the steel cup was preheated to 300 °C. The temperature data was collected by a data acquisition system (National Instruments NI-9211) linked to a personal computer at a 4 Hz sampling frequency.

Vzorce RPT (pretaljene in tradicionalne) smo prerezali na pol in jih zbrusili z brusnimi papirji SiC z zrnatostjo 180, 320 in 500. S skenerjem smo naredili slike prečnega prereza z ločljivostjo 1000 dpi, nato pa smo za analizo slik uporabili programsko opremo MATLAB Image Processing Toolbox™ (kot je opisano v referenci [32]). Pore s površino, manjšo od 30 pik (0,0194 mm^2), niso bile upoštevane. Za mikrostrukturno analizo smo vzorce dodatno zbrusili do zrnatosti 2400 in jih spolirali z diamantno suspenzijo velikosti 3 in 1 µm. Izvedene so bile meritve razdalje med sekundarnimi dendritnimi vejami (SDAS). Povprečna razdalja SDAS je bil ocenjena z mikrografijami prečnih prerezov pretaljenih in tradicionalnih vzorcev RPT. Za vsak vzorec je bilo opravljenih 20 meritev v 4 različnih vidnih poljih (80 meritev/vzorec).

Na podlagi rezultatov analize slik je bil izračunan indeks bifilma (BI [mm]) kot [33]:

$$BI = \sum L_{max}\,, \qquad \text{En. 1}$$

kjer je L_{max} največja dolžina (dolžina glavne osi) por [mm]. Bifilm-Index, normaliziran na površino vzorca (NBI [mm/cm^2]), je bil ocenjen kot:

$$NBI = \frac{\sum L_{max}}{A_{Sample}}\,, \qquad \text{En. 2}$$

kjer je A_{sample} [cm^2] površina prečnega prereza vzorcev. Gostota števila por (N_d [cm^{-2}]):

$$N_d = \frac{N}{A_{Sample}} \qquad \text{En. 3}$$

kjer je N [-] skupno število por. Delež površine por (A_f [%]):

$$A_f = \frac{\sum A_P}{A_{Sample}} \cdot 100 \qquad \text{En. 4}$$

kjer je A_p [cm^2] površina pore. Poleg tega je bil izračunan tudi normalizirani skupni obseg por (NTPP) [mm/cm^2]:

$$NTPP = \frac{\Sigma P_P}{A_{Sample}} \qquad \text{En. 5}$$

kjer je P_P [mm] obseg pore. Faktor oblike (S_F) por je bil izračunan kot [33]:

The RPT samples (both remelted and traditional) were cut in half and ground with SiC grinding papers with grit sizes 180, 320, and 500. A scanner was used to make cross-sectional images with 1000 dpi resolution, and then the MATLAB Image Processing Toolbox™ software was used for image analysis (as described in ref. [32]). Pores with an area smaller than 30 pixels (0.0194 mm^2) were not taken into account. For microstructural analysis, samples were further ground up to 2400 grit size and polished with 3 and 1 µm diamond suspensions. Secondary dendrite arm spacing (SDAS) measurements were conducted. The average SDAS was evaluated by micrographs made from the cross-sections of remelted and traditional RPT samples. For each specimen, 20 measurements were made in 4 different fields of view (80 measurements/sample).

Based on the results of the image analysis, Bifilm-Index (BI [mm]) was calculated as [33]:

$$BI = \sum L_{max}\,, \qquad \text{Eq. 1}$$

where L_{max} is the maximum length (major axis length) of pores [mm]. Bifilm-Index normalized to sample area (NBI [mm/cm^2]) was evaluated as:

$$NBI = \frac{\sum L_{max}}{A_{Sample}}\,, \qquad \text{Eq. 2}$$

where A_{sample} [cm^2] is the cross-sectional area of the samples. The pore number density (N_d [cm^{-2}]):

$$N_d = \frac{N}{A_{Sample}} \qquad \text{Eq. 3}$$

where N [-] is the total number of pores. The pore area fraction (A_f [%]):

$$A_f = \frac{\sum A_P}{A_{Sample}} \cdot 100 \qquad \text{Eq. 4}$$

where A_p [cm^2] is the area of a pore. Additionally, the normalized total pore perimeter (NTPP) [mm/cm^2] was also calculated as:

$$S_F = \frac{4\pi A_P}{P_p^2} \qquad \text{En. 6}$$

pri čemer bi bil S_F popolnega kroga enak 1.

4 Rezultati in razprava

4.1 Simulacije strjevanja

Slika 6 prikazuje simulirane temperaturne porazdelitve na prečnih prerezih tradicionalnih **(Slika 6 (a))** in pretaljenih vzorcev RPT **(Slika 6 (b, c))** v različnih fazah strjevanja. **Slika 6. (b)** prikazuje primer, ko je bilo kot porozni medij uporabljenih 55 g, in **Slika 6. (c),** ko je bilo kot porozni medij uporabljenih 30 g kremenčevega peska. V vseh primerih je bila začetna temperatura taline 700 °C v skladu z eksperimentalnimi parametri. Vendar je bila temperatura orodja precej drugačna: jeklena čaša tradicionalnega vzorca RPT je bila nastavljena na 300 °C, medtem ko sta bila peščena podpora in jeklena čaša pretaljenih vzorcev nastavljena na 700 °C.

Slika 7 povzema lokalne čase strjevanja **(Slika 7. (a-c))** in čase strjevanja **(Slika 7. (d-f))** na prečnih prerezih vzorcev. Lokalni čas strjevanja (t_f [s]) je opredeljen kot čas, ki je potreben na danem mestu v ulitku, da temperatura pade z likvidus na neuravnoteženo solidus temperaturo, medtem ko se čas strjevanja (t_{sol} [s]) razume kot čas, ki je potreben na danem mestu v ulitku, da temperatura pade s temperature ulitka na neuravnoteženo solidus temperaturo. Skupni čas strjevanja (t_{total} [s]) je čas, potreben za doseganje 0 % deleža tekoče faze v celotnem ulitku od trenutka ulivanja. Pretaljeni vzorci se začnejo strjevati pozneje kot tradicionalni vzorci RPT, kar je posledica predgretega peščenega polnila. V primeru uporabe 55 g peska se pod vzorcem ustvari vroče mesto **(Slika 6 (b)),** kar podaljša čas strjevanja in

$$NTPP = \frac{\Sigma P_P}{A_{Sample}} \qquad \text{Eq. 5}$$

where P_P [mm] is the perimeter of a pore. The shape factor (S_F) of the pores was calculated as [33]:

$$S_F = \frac{4\pi A_P}{P_p^2} \qquad \text{Eq. 6}$$

where a perfect circle would have an S_F of 1.

4 Results and discussion

4.1 Solidification simulations

Figure 6 shows the simulated temperature distributions at the cross sections of traditional **(Figure 6 (a))** and remelted RPT samples **(Figure 6 (b, c))** at different stages of the solidification. **Figure 6 (b)** presents the case when 55 g and **Figure 6. (c)** when 30 g of silica sand was used as a porous medium. In all cases, the starting temperature of the liquid metal was 700 °C in accordance with the experimental parameters. The mold temperature, however, was rather different: the steel cup of the traditional RPT sample was set to 300 °C, while the sand support and steel cup of the remelted specimens were set to 700 °C.

Figure 7 summarizes the local solidification times **(Figure 7 (a-c))** and solidification times **(Figure 7 (d-f))** at the cross sections of the samples. Local solidification time (t_f [s]) is defined as the time taken at a given location in a casting for the temperature to fall from the liquidus to the non-equilibrium solidus, while solidification time (t_{sol} [s]) is interpreted as the time needed at a given location in a casting for the temperature to fall from the casting temperature to the non-equilibrium solidus. The total solidification time (t_{total} [s]) is the time needed to reach 0 % liquid phase fraction in the whole casting, starting from the moment of casting. The

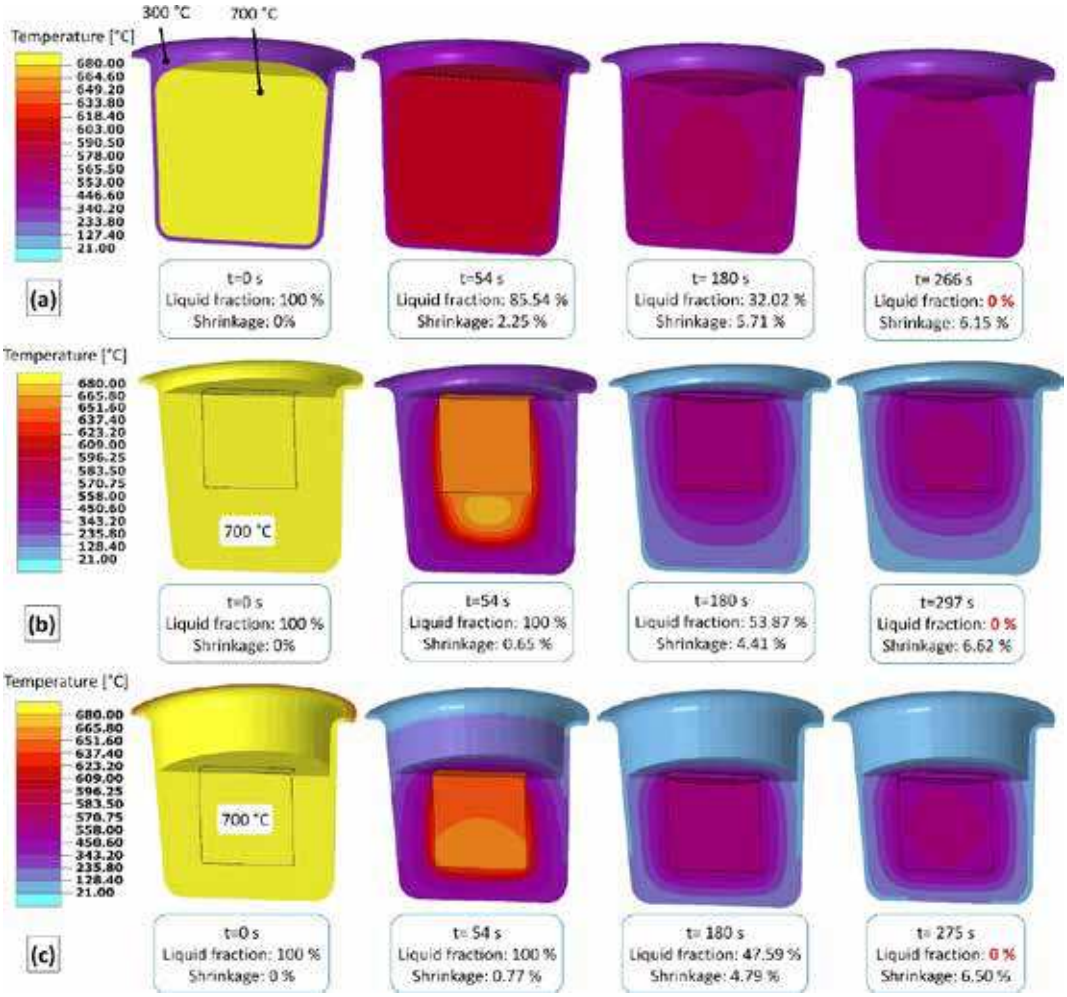

Slika 6. Prečni prerez porazdelitve temperature glede na simulacije strjevanja (a) tradicionalnih in (b,c) pretaljenih vzorcev RPT v različnih fazah procesa strjevanja. (b) predstavlja primer, ko je bilo za talilno sredstvo uporabljenih 55 g in (c), ko je bilo uporabljenih 30 g kremenčevega peska

Figure 6. Cross-sectional view of the temperature distribution according to solidification simulations of (a) traditional and (b, c) remelted RPT samples at different stages of the solidification process. (b) presents the case when 55 g and (c) when 30 g of silica sand was used as a melting medium

povzroči, da je skupni čas strjevanja 297 s **(Slika 7 (e)).** Po drugi strani pa je pri uporabi 30 g peska kot polnila skupni čas strjevanja precej podoben kot pri tradicionalnem RPT (z razliko 9 s).

Čeprav so skupni časi strjevanja tradicionalnih vzorcev RPT in vzorcev, remelted samples start to solidify later than the traditional RPT specimen, which is a consequence of the preheated sand filling. In the case of using 55 g sand, a hot spot is formed under the specimen **(Figure 6 (b)),** which increases the solidification time and results in a total solidification time of 297 s

pretaljenih v 30 g peska, precej podobni, je lokalni čas strjevanja pri pretaljenem kosu izrazito krajši **(Slika 7 (c)).** Ker je finost mikrostrukture odvisna od lokalnega časa strjevanja, bi bila zgolj na podlagi simulacij uporaba 55 g peska boljša izbira v smislu zagotavljanja podobnih pogojev strjevanja kot v primeru tradicionalnega vzorca RPT. Po drugi strani pa so predhodni preskusi pokazali, da se pri uporabi posodic za vzorčenje, popolnoma napolnjenih s peskom, mehurčki na vrhu vzorcev zaradi zapoznelega začetka postopka strjevanja bolj razpočijo. Zato je bilo med dejanskimi poskusi uporabljenih 30 g peščenega polnila.

4.2 Analiza mikrostrukture in termična analiza

Da bi ugotovili, ali so bili lokalni časi strjevanja pretaljenih vzorcev res podobni kot pri tradicionalnih vzorcih RPT, smo izvedli meritve razdalje SDAS. Ocenjevanje SDAS je koristno orodje, ki se lahko uporablja za napovedovanje lokalnih časov strjevanja različnih zlitin [34–36]. Povprečna razdalja SDAS je bila izračunana z meritvami, **(Figure 7.(e))**. On the other hand, applying 30 g of sand as a filler results in a rather similar total solidification time as in the case of the traditional RPT (with a 9 s difference).

Although the total solidification times of traditional RPT specimens and samples remelted in 30 g sand are rather similar, the local solidification time is remarkably less for the remelted piece **(Figure 7 (c)).** As the fineness of the microstructure is controlled by the local solidification time, based solely on the simulations, using 55 g sand would be a better choice in terms of providing similar solidification conditions as in the case of traditional RPT. On the other hand, preliminary tests revealed that using sampling cups filled fully with sand results in a more significant bubble bursting at the top of the samples due to the delayed start of the solidification process. For this reason, 30 g of sand filling was used during real-life experiments.

4.2 Microstructural investigation and thermal analysis

To investigate whether the local solidification times of remelted samples were indeed similar to those of the traditional RPT

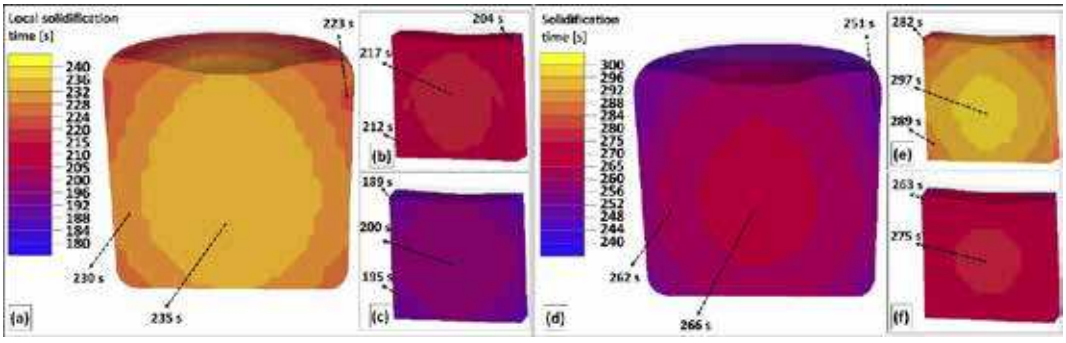

Slika 7. (a-c) Lokalni časi strjevanja in (d-f) s časi strjevanja na prerezih (a, d) tradicionalnih vzorcev RPT in vzorcev, pretaljenih v (b, e) 55 g in (c, f) 30 g kremenčevega peska

Figure 7. (a-c) Local solidification times and (d-f) solidification times at the cross-sections of (a, d) traditional RPT specimens and samples remelted in (b, e) 55 g and (c, f) 30 g silica sand

opravljenimi na mikrografih pretaljenih **(Slika 8 (a, c))** in tradicionalnih vzorcev RPT **(Slika 8 (b, d)).** V vsakem primeru je povprečna razdalja SDAS približno 50 µm z zanemarljivim odstopanjem, kar pomeni, da razlike v lokalnih časih strjevanja, ki jih kažejo simulacije, nimajo bistvenega vpliva na razdalje med sekundarnimi dendritnimi vejami vzorcev.

Podobno kot pri simulacijah tudi rezultati termične analize kažejo na precejšnjo razliko v lokalnih časih strjevanja (približno 56 s), medtem ko je razlika v skupnih časih strjevanja manjša **(Slika 9).** Opozoriti je treba, da bi lahko bila razlika med strjevanjem brez termočlenov manjša, saj lahko termočlen odvede nekaj toplote, ta učinek pa je pomembnejši v primeru majhnega pretaljenega vzorca.

samples, SDAS measurements were conducted. Evaluating SDAS is a useful tool that can be used for the prediction of local solidification times of different alloys [34-36]. The average SDAS was calculated by measurements made on micrographs taken from remelted **(Figure 8 (a, c))** and traditional RPT samples **(Figure 8 (b, d))**. In each case, the average SDAS is around 50 µm with negligible variation, which means the differences in the local solidification times indicated by the simulations do not have a significant effect on the secondary dendrite arm spacings of the samples.

Similarly to the simulations, the thermal analysis results also indicate a remarkable difference in the local solidification times (approximately 56 s), whereas there is a smaller difference in total solidification times **(Figure 9)**. It should be noted that the difference could be less significant during

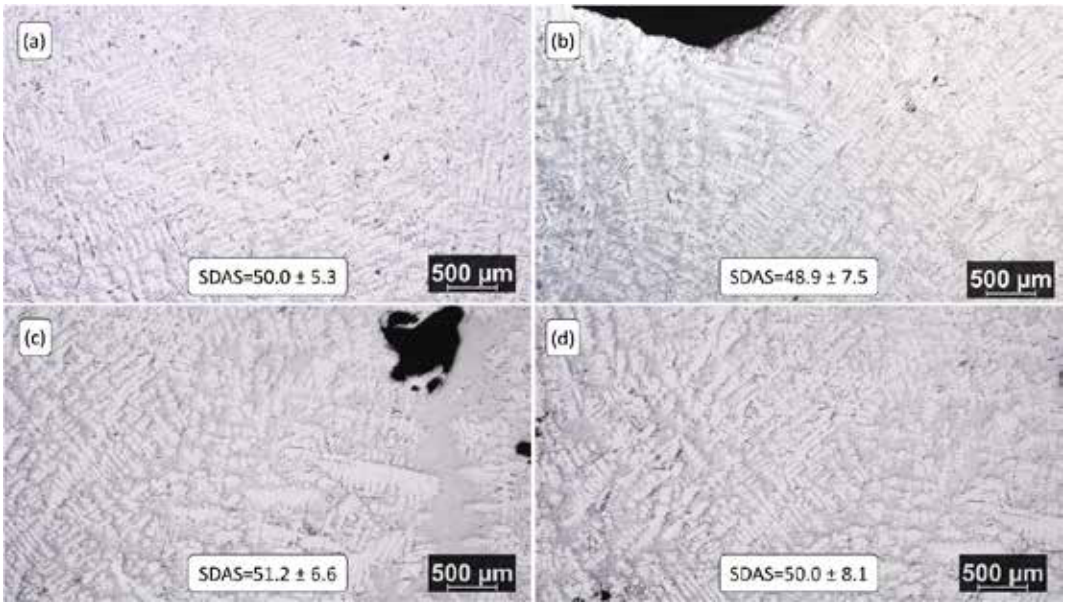

Slika 8. Slike mikrostrukture preiskovanih vzorcev: (a) pretaljen ulitek HDC, (b) tradicionalni ulitek HDC, (c) pretaljen gravitacijski ulitek in (d) gravitacijski tradicionalni ulitek

Figure 8. Microstructural images of the investigated samples: (a) HDC cast remelted, (b) HDC cast traditional, (c) gravity cast remelted, and (d) gravity cast traditional

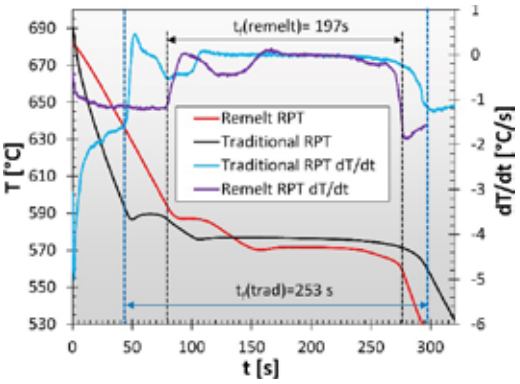

Figure 9. Cooling curves of traditional and remelt RPT samples

Slika 9. Krivulje ohlajanja tradicionalnih in pretaljenih vzorcev RPT

Znano je, da lahko razmik med sekundarnimi dendritnimi vejami (SDAS [m]) ocenimo iz lokalnih časov strjevanja (t_f [s]) po naslednji formuli [37]:

$$SDAS = K\left(Mt_f\right)^{1/3} \qquad \text{En. 7}$$

kjer je

$$M = -\frac{\Gamma D}{m\left(1-k\right)\left(c_E - c_0\right)}\ln\left(\frac{c_E}{c_0}\right) \qquad \text{En. 8}$$

K je numerična konstanta, ki po *Feurerju* in *Wunderlinu* [38] znaša 5,5, in $128^{1/3} \approx 5{,}0$ po *Kirkwoodu* [39]. Γ je Gibbs-Thomsonov koeficient [K·m], D je difuzivnost atomov topljenca v tekočini [m^2/s], C_E pomeni evtektično sestavo (12,6 mas. % v sistemu Al-Si), C_0 je koncentracija topljenca (9 masnih %), m je naklon krivulje likvidusa (6,6 °C/mt. % za Al-Si) in k je porazdelitveni koeficient, ki znaša 0,13 za Si v Al [34]. Γ je podan kot

$$\Gamma = \frac{\sigma_{SL}}{\Delta S_f} \qquad \text{En. 9}$$

kjer je σ_{SL} medfazna energija trdne in tekoče snovi [J/m^2], ΔS_f je entropija zlivanja [$J/K{\cdot}m^3$]. Če uporabimo σ_{SL} = 0,15 J/m^2 [40] in $\Delta S_f = 1{,}112{\cdot}10^6$ $J/K{\cdot}m^3$ [41], je Γ $1{,}349{\cdot}10^{-7}$ K·m. Če je D = $2{,}05{\cdot}10^{-9}$ m^2/s solidification without thermocouples, as some heat may be conducted away by the thermocouple, which has a more significant effect in the case of the small-sized remelted sample.

It is well-known that the secondary dendrite arm spacing (SDAS [m]) can be estimated from the local solidification times (t_f [s]) according to the following formula [37]:

$$SDAS = K\left(Mt_f\right)^{1/3} \qquad \text{Eq. 7}$$

where

$$M = -\frac{\Gamma D}{m\left(1-k\right)\left(c_E - c_0\right)}\ln\left(\frac{c_E}{c_0}\right) \qquad \text{Eq. 8}$$

K is a numerical constant, which is 5.5 according to *Feurer* and *Wunderlin* [38], and $128^{1/3} \approx 5.0$ according to *Kirkwood* [39]. Γ is the Gibbs-Thomson coefficient [K·m], D is the diffusivity of solute atoms in liquid [m^2/s], C_E denotes the eutectic composition (12.6 wt. % in the Al-Si system), C_0 is the solute concentration (9 wt. %), m is the slope of the liquidus curve (6.6 °C/wt. % for Al-Si), and k is the distribution coefficient, which is 0.13 for Si in Al [34]. Γ is given as

$$\Gamma = \frac{\sigma_{SL}}{\Delta S_f} \qquad \text{Eq. 9}$$

where σ_{SL} is the solid/liquid interfacial energy [J/m^2], ΔS_f is the entropy of fusion [$J/K{\cdot}m^3$]. Using σ_{SL} = 0.15 J/m^2 [40] and $\Delta S_f = 1.112{\cdot}10^6$ $J/K{\cdot}m^3$ [41], Γ is $1.349{\cdot}10^{-7}$ K·m. If D = $2.05{\cdot}10^{-9}$ m^2/s (which was calculated at 590 °C liquidus temperature based on ref. [42]), the experimentally measured 50 µm SDAS is given by **Eq. 7** at 223 s when 5.0 and 167 s when 5.5. By comparing the measured and calculated local solidification times **(Table 2)**, the matching between the values is relatively good when the numerical constant of *Kirkwood* [39] is used. Also, it is worth noting that the local and total solidification times acquired by solidification simulations are also in accordance with the experimental results. Based on the

(kar je bilo izračunano pri temperaturi 590 °C likvidusa na podlagi literature [42]), je eksperimentalno izmerjeni 50 µm SDAS podan z **enačbo 7** pri 223 s, ko je 5,0, in 167 s, ko je 5,5. Če primerjamo izmerjene in izračunane lokalne čase strjevanja **(Preglednica 2),** ugotovimo, da se vrednosti razmeroma dobro ujemajo, če uporabimo številčno konstanto *Kirkwooda* [39]. Prav tako je treba omeniti, da so tudi lokalni in skupni časi strjevanja, pridobljeni s simulacijami strjevanja, v skladu z eksperimentalnimi rezultati. Na podlagi zgoraj opisanih rezultatov lahko rečemo, da obstajajo nekatere razlike med lokalnimi časi strjevanja tradicionalnih in pretaljenih vzorcev RPT, vendar so te razlike premajhne, da bi jih bilo mogoče dokazati z analizo mikrostruktur. To pomeni, da razlike v lokalnih hitrostih strjevanja ne vplivajo bistveno na nastanek por.

Preglednica 2. Primerjava izmerjenih in izračunanih časov strjevanja

Table 2. Comparison of measured and calculated solidification times

Parameter / Parameter	Tradicionalni / Traditional RPT	Pretaljeni / Remelted RPT
t_f (izmerjeno s / measured by TA) [s]	253	197
t_f (simulirano / simulated) [s]	223–235	189–200
t_f (izračunano iz / calculated from SDAS, Kirkwood [39]) [s]	223	
t_f (izračunano iz SDAS, Feurer in Wunderlin [38]) [s]	167	
t_{total} (izmerjeno s / measured byTA) [s]	297	276
t_{total} (simulirano / simulated) [s]	266	275

4.3 Ocena kakovosti

V **Preglednici 3** so povzeti rezultati analize slik pretaljenih vzorcev RPT, na **Sliki 10** pa je prikazana primerjava posameznih parametrov, ocenjenih med analizo. Na results detailed above, it can be said that there are some differences between the local solidification times of traditional and remelted RPT samples, but these differences are too small to be evinced by microstructural investigations. This means that pore formation is not notably affected by the differences in the local solidification rates.

4.3 Quality evaluation

Table 3 summarizes the image analysis results of remelted RPT samples, while **Figure 10.** shows the comparison of the individual parameters evaluated during the analysis. **Figure 11.** summarizes the distribution of maximum pore diameters **(Figure 11. (a, b))** and shape factors **(Figure 11. (c, d))** of the pores found within the 10 DC and 10 GC remelted samples. The compiled results in **Table 3** show clear differences between the porosity parameters of the specimens extracted from the ingots cast by the two technologies: the gravity cast ingot possesses higher values, which indicates higher impurity content. The average pore area fraction is almost double, and the average BI is more than one and a half times the values of the direct-chill cast ingot. Based on this, the bifilm and gas content (solute hydrogen and entrained air) of the gravity cast ingot is remarkably higher, which is in agreement with the results of *Erzi* and *Tiryakioğlu* [24], who found that the quality of DC cast AlSi7Mg0.3 ingots was more favorable than that of the gravity cast ingots. According to *Uludağ* et al. [43], the melt quality can be categorized by the BI values as follows:

- 0 mm ≤ BI ≤ 10 mm: high-quality melt,
- 10 mm ≤ BI ≤ 25 mm: good quality,
- 25 mm ≤ BI ≤ 50 mm: average quality,
- 50 mm ≤ BI ≤ 100 mm: unacceptable

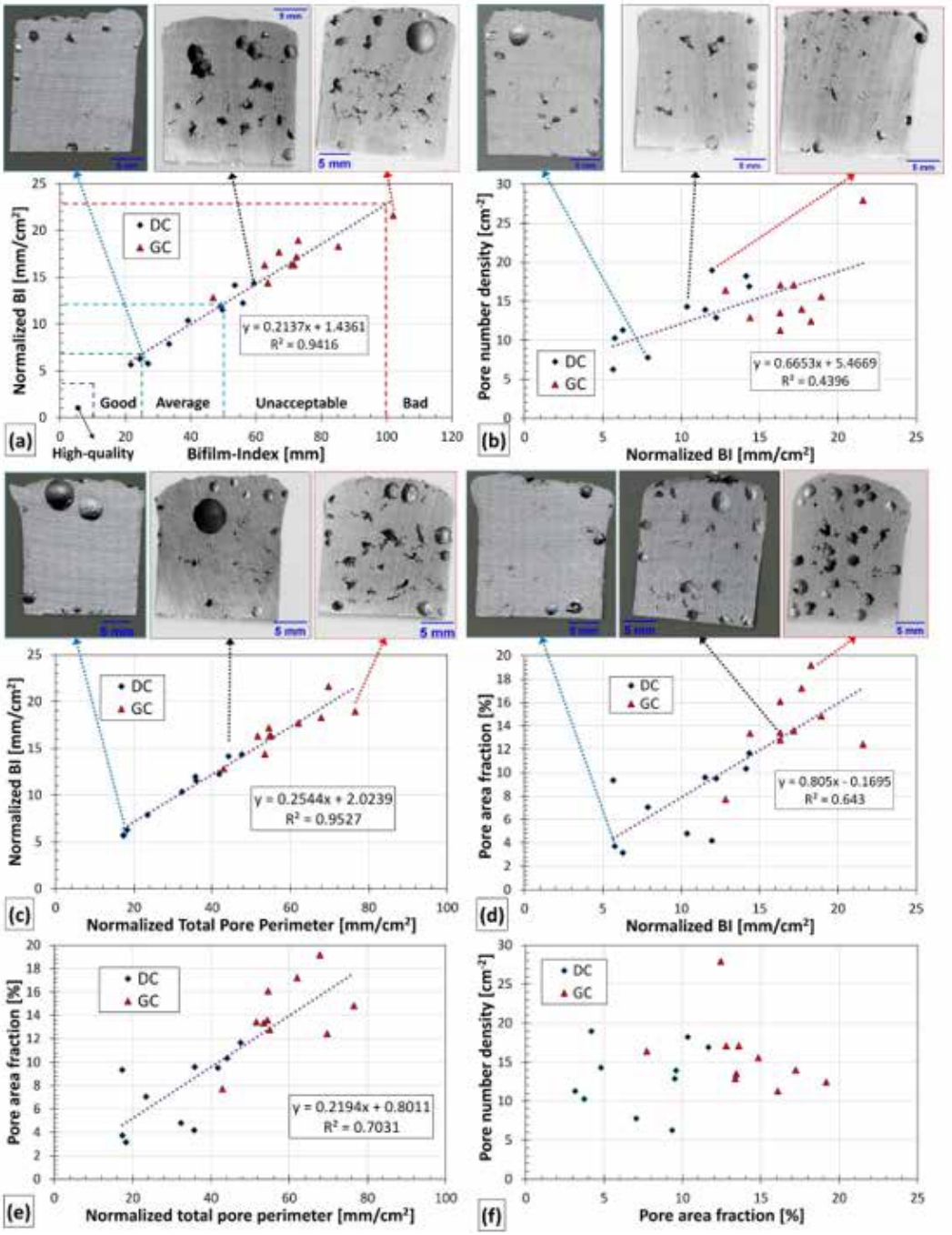

Slika 10. (a-f) Primerjava različnih parametrov, ocenjenih s slikovno analizo pretaljenih vzorcev (DC: polkontinuirano ulivanje, GC: gravitacijsko litje ingota)

Figure 10. (a-f) Comparison of different parameters evaluated by the image analysis of remelted samples (DC: direct-chill cast, GC: gravity cast ingot)

Sliki 11 je povzeta porazdelitev največjih premerov por **(Slika 11 (a, b))** in koeficientov oblike **(Slika 11. (c, d))** por, najdenih v 10 vzorcih DC in 10 vzorcih GC, ki so bili pretaljeni. Rezultati, zbrani v **Preglednici 3**, kažejo jasne razlike med parametri poroznosti vzorcev, pridobljenih iz ingotov, ulitih z obema tehnologijama: gravitacijsko ulit ingot ima višje vrednosti, kar kaže na večjo vsebnost nečistoč. Povprečni delež površine por je skoraj dvakrat večji, povprečni indeks BI pa več kot enkrat in pol večji od vrednosti polkontinuirano ulitega ingota. Na podlagi tega je vsebnost bifilma in plinov (raztopljenega vodika in zajetega zraka) v gravitacijsko ulitem ingotu izrazito višja, kar je v skladu z rezultati *Erzija* in *Tiryakioğluja* [24], ki sta ugotovila, da je kakovost ingotov AlSi7Mg0.3, ulitih z DC, ugodnejša od kakovosti gravitacijsko ulitih ingotov. Po *Uludağu* in drugih [43] je kakovost taline mogoče razvrstiti v naslednje kategorije glede na vrednosti indeksa BI:

- 0 mm ≤ BI ≤ 10 mm: visokokakovostna talina,
- 10 mm ≤ BI ≤ 25 mm: dobra kakovost,
- 25 mm ≤ BI ≤ 50 mm: povprečna kakovost,
- 50 mm ≤ BI ≤ 100 mm: nesprejemljiva kakovost,
- BI ≥ 100 mm: slaba kakovost, ki se ji je treba izogniti.

quality,

- BI ≥ 100 mm: bad quality that should be avoided.

Based solely on this scale, the DC cast ingot falls into the „average quality" category, while the gravity cast ingot belongs to the „unacceptable quality" category. However, it should be emphasized that the remelted samples of this study have a smaller cross-section than traditional RPT samples, which were presumably used for the establishment of the quality scale of *Uludağ* et al, so even stricter BI limits should be used for the categorization in our case. There are several studies [22, 44-49] that showed that BI values correlate with mechanical properties, which means that the mechanical properties of castings made from the two investigated types of ingots could differ (using the same technological parameters). This presumption will be investigated in a future study.

Because the cross-sectional area of the samples was relatively constant, there is a strong correlation between BI and NBI values **(Figure 10. (a))**. By comparing pore number density and NBI results **(Figure 10. (b))**, we only found a poor correlation, which is in accordance with the results of *Uludağ* et al. [43], but somewhat contradicts the results of *Dispina*r and *Campbell* [44, 49] who found a strong linear correlation

Preglednica 3. Rezultati analize slik pretaljenih vzorcev

Table 3. Image analysis results of remelted samples

Parameter / Parameter	Polkontinuirano ulivanje / Direct-chill cast (DC)	Gravity cast / Gravitacijsko litje (GC)
Delež površine por / Pore area fraction (Af) [%]	7.33±3.14	14.07±3.10
Gostota števila por / Pore number density (Nd) [cm^{-2}]	13.07±4.26	15.82 ± 4.71
Normalizirani skupni obseg por / Normalized total pore perimeter (NTPP) [mm/cm^2]	31.40±11.55	58.81±10.04
Bifilm-Index (BI) [mm]	41.37±14.02	71.55±14.50
Normalizirani indeks bifilma / Normalized Bifilm-Index (NBI) [mm/cm^2]	10.01±3.38	16.99±2.42

Zgolj na podlagi te lestvice sodi DC-ulit ingot v kategorijo »povprečne kakovosti«, medtem ko gravitacijsko ulit ingot spada v kategorijo »nesprejemljive kakovosti«. Vendar je treba poudariti, da imajo pretaljeni vzorci te študije manjši prečni prerez kot tradicionalni vzorci RPT, ki so bili domnevno uporabljeni za določitev lestvice kakovosti *Uludağa* in drugih, zato je treba v našem primeru za kategorizacijo uporabiti še strožje meje indeksa BI. Več študij [22, 44–49] je pokazalo, da vrednosti BI korelirajo z mehanskimi lastnostmi, kar pomeni, da bi se lahko mehanske lastnosti ulitkov, izdelanih iz obeh preučevanih vrst ingotov, razlikovale (ob uporabi enakih tehnoloških parametrov). To domnevo bomo preučili v prihodnji študiji.

Ker je bila površina prečnega prereza vzorcev razmeroma konstantna, obstaja močna korelacija med vrednostmi BI in NBI **(Slika 10 (a)).** S primerjavo gostote števila por in rezultatov NBI **(Slika 10 (b))** smo ugotovili le slabo korelacijo, kar je v skladu z rezultati *Uludağa* in drugih [43], vendar nekoliko nasprotuje rezultatom *Dispinarja* in *Campbella* [44, 49], ki sta ugotovila močno linearno korelacijo med številom por in vrednostmi BI za različne zlitine. Vendar je treba opozoriti, da število por in skupni premer por (BI) nista nujno medsebojno povezana. Močna korelacija je pričakovana, kadar ima večina por podoben premer. Teoretično pa lahko enak indeks BI dosežemo s številnimi majhnimi porami ali z nekaj večjimi porami. Če si ogledamo slike prečnega prereza na **Sliki 10 (a-d)** lahko vidimo, da so v nekaterih primerih razlike v velikosti por velike, kar pojasnjuje slabo korelacijo na **Sliki 10 (b).** Poročali so, da v večini primerov premer por v vzorcih RPT sledi lognormalni porazdelitvi [43, 50] in da ima večina por podoben premer, kar pomeni, da lahko pričakujemo neko vrsto korelacije med številom por in indeksom

between the number of pores and BI values for different alloys. However, it is worth noting that the number of pores and total pore diameter (BI) are not necessarily interrelated. A strong correlation is expected when most of the pores have similar diameters. However, in theory, the same BI can be reached with numerous small pores or with a few larger ones. By looking at the cross-sectional images in **Figure 10 (a-d)**, it can be seen that there are cases when the differences in the sizes of the pores are remarkable, which explains the poor correlation in **Figure 10 (b)**. It was reported that in most cases, the diameter of the pores in RPT samples follows the lognormal distribution [43, 50], and it is common that most of the pores have a similar diameter, which means that some type of correlation between the number of pores and BI can be expected. However, there could be circumstances that can contribute to non-uniform pore size distribution, as it was reported by *LaOrchan* et al. [51]. In the case of short-freezing range alloys (like 413), a solid shell may form on the surface of the RPT sample, which can result in a large central pore caused by shrinkage. In our case, the distribution of maximum pore diameters **(Figure 11 (a, b)** show that most of the pores fall into the size range of 0.2-0.4 mm for both HDC and GC samples. However, there is a significant fraction within the size range of 1-2 mm, especially in the case of GC specimens, which explains the poor fitting in **Figure 10 (b)**.

There is an excellent linear correlation between NBI and NTPP with an R^2 value of 0.9527 **(Figure 10. (c))**. It was reported by *Uludağ* et al. [43] that there is a strong relationship between the total volume of pores and BI. However, a relationship between the total pore perimeter (and its normalized values) and BI has not been published yet. *Dispinar* and *Campbell*

BI. Vendar pa lahko obstajajo okoliščine, ki lahko prispevajo k neenakomerni porazdelitvi velikosti por, kot so poročali *LaOrchan* in drugi [51]. Pri zlitinah s kratkim območjem strjevanja (kot je 413) lahko na površini vzorca RPT nastane trdna lupina, ki lahko povzroči veliko osrednjo poro zaradi krčenja. V našem primeru porazdelitev največjih premerov por **(Slika 11. (a, b)** kaže, da je večina por v območju velikosti 0,2–0,4 mm pri vzorcih HDC in GC. Vendar pa je precejšen delež v območju

[52] highlighted that the maximum pore diameter is an approximation of the bifilm length. Based on this assumption, the main idea behind NTPP is that pore perimeter can be used as a rough 2-dimensional approximation of bifilm surface area (naturally, it is an overestimate as bifilms are expanded during solidification). From this point of view, NTPP is a 2-dimensional version of the Bifilm Spatial Index (BSI) introduced by *Song* et al. [53]. If we assume that each pore has a perfectly circular cross-section, the relationship between

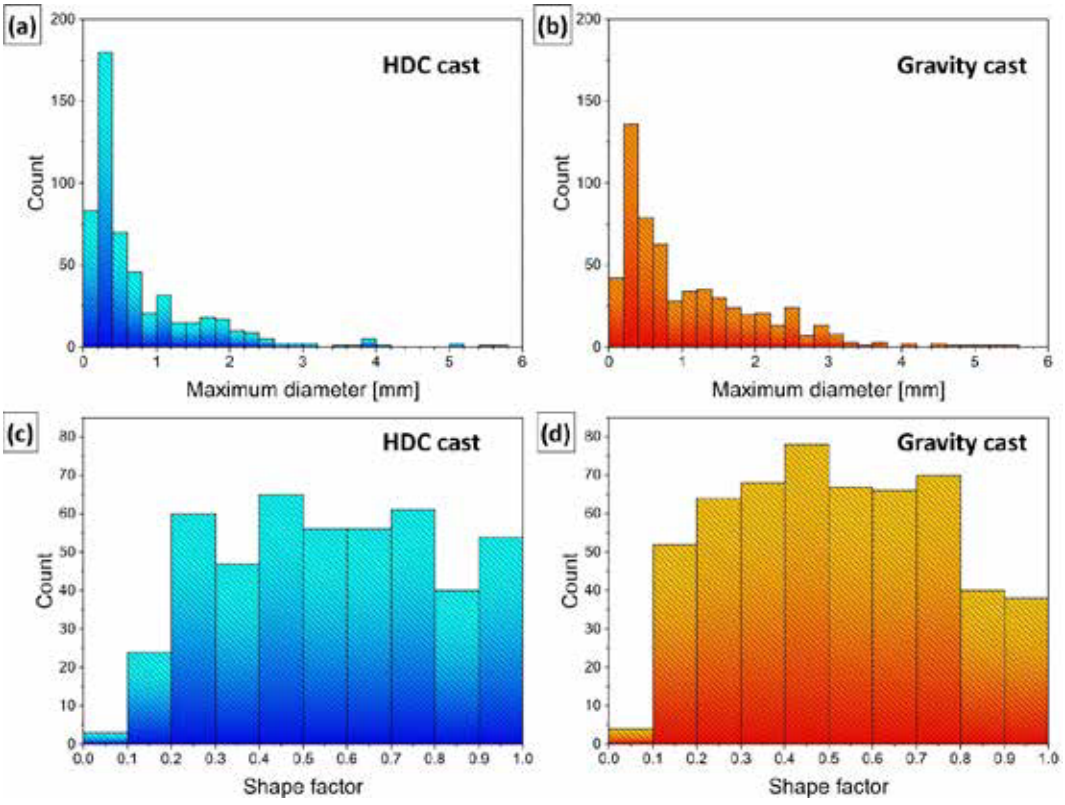

Slika 11. Porazdelitev (a, b) največjih premerov por (c, d) in koeficientov oblike por v (a, c) vzorcih HDC in (b, c) gravitacijsko litih vzorcih. Pri analizi so bili združeni podatki o porah 10-10 pretaljenih vzorcev.

Figure 11. Distribution of (a, b) maximum pore diameters (c, d) and pore shape factors in (a, c) HDC and (b, c) gravity cast samples. For the analysis, the pore data of the 10-10 remelted samples were merged

velikosti 1–2 mm, zlasti pri vzorcih GC, kar pojasnjuje slabo prileganje na **Sliki 10. (b).**

Med NBI in NTPP obstaja odlična linearna korelacija z vrednostjo R^2 0,9527 **(Slika 10. (c)).** *Uludağ* in drugi [43] so poročali, da obstaja močna povezava med skupno prostornino por in indeksom bifilma. Vendar razmerje med skupnim obsegom por (in njegovimi normaliziranimi vrednostmi) in indeksom BI še ni bilo objavljeno. *Dispinar* in *Campbell* [52] sta poudarila, da je največji premer por približek dolžine bifilma. Na podlagi te predpostavke je vodilna ideja pri NTPP, da se obseg por lahko uporabi kot grob dvodimenzionalni približek površine bifilma (seveda gre za precenjeno oceno, saj se bifilmi med strjevanjem razširijo). S tega vidika je NTPP dvodimenzionalna različica prostorskega indeksa bifilma (BSI), ki so ga predstavili *Song* in drugi [53]. Če predpostavimo, da ima vsaka pora popolnoma okrogel prečni presek, bi moralo biti razmerje med skupnim obsegom por in indeksom BI (ter njunimi normaliziranimi vrednostmi) preprosto faktor, ki je enak vrednosti π **(Slika 12. (a)).** V tem primeru bi moral biti π^{-1} = 0,3183-kratnik NTPP. Če prestavimo regresijsko premico, da preseka os ordinato pri vrednosti 0, dobimo razmerje, ki je precej blizu teoretičnemu: NBI = 0,2937NTPP. Razlika je predvsem posledica dejstva, da pore niso popolnoma sferične in da njihovi prečni preseki niso popolnoma okrogli. Na **Sliki 12 (a)** lahko vidimo, da se vrednosti vzorcev GC bolj razlikujejo od teoretičnega razmerja, kar pomeni, da so pore v teh vzorcih manj sferične. To potrjujejo podatki o koeficientu oblike na **Sliki 11 (c, d),** ki kaže, da je v vzorcih HDC, ki imajo koeficient oblike med 0,9 in 1,0, več por. Povprečni koeficient oblike por v vzorcih HDC in GC je 0,65 oziroma 0,57.

Rezultati deleža površine por slabo korelirajo z normaliziranim indeksom BI

the total pore perimeter and BI (and their normalized values) should be simply a factor equal to the value of π **(Figure 12. (a))**. In this case, NBI should be π^{-1}=0.3183 times NTPP. If we force the regression line to intercept the axis of ordinates at 0, we get a relationship, which is pretty close to the theoretical one: NBI=0.2937NTPP. The difference is mainly caused by the fact that pores are not perfectly spherical, and their cross-sections are not perfectly circular. We can see in **Figure 12. (a)** that the values of GC samples differ more significantly from the theoretical relationship, meaning that the pores are less spherical in these specimens. This is supported by the shape factor data in **Figure 11 (c, d)**, which shows that there are more pores in HDC samples, which have a shape factor between 0.9 and 1.0. The average shape factor of the pores found in HDC and GC specimens is 0.65 and 0.57, respectively.

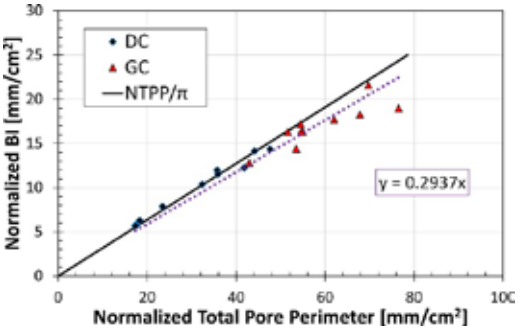

Slika 12. Razmerje med NBI in NTPP v teoretičnem primeru, ko so pore popolnoma sferične (črna črta), v primerjavi z eksperimentalnimi podatki

Figure 12. Relationship between NBI and NTPP in the theoretical case, when the pores are perfectly spherical (black line), compared with the experimental data

The pore area fraction results correlate poorly with normalized BI **(Figure 10. (d))** and NTPP **(Figure 10. (e))**, which can also

(Slika 10 (d)) in NTPP **(Slika 10 (e)),** kar je mogoče razložiti tudi z odstopanjem por od sferične oblike. Med gostoto števila por in deležem površine por ni bila ugotovljena povezava **(Slika 10 (f)).** Upoštevajte, da bi moralo teoretično vsako razmerje, predstavljeno na **Sliki 10,** presekati ordinatno os pri vrednosti 0. Da bi dobili reprezentativne vrednosti R^2, regresijske premice niso morale biti presečne pri vrednosti 0.

4.4 Tradicionalni vzorci RPT

Rezultati analize slik tradicionalnih vzorcev RPT **(Slika 13),** ulitih iz pretaljenih delov ingotov, kažejo podobno razliko med polkontinuirano ulitimi ingoti in gravitacijsko ulitimi ingoti, kot je prikazano v **Preglednici 3**. Skoraj vsi preučeni parametri so višji pri vzorcih gravitacijsko ulitih ingotov **(Slika 13 (a)),** kar kaže na večjo vsebnost bifilma in plina. Edina izjema je gostota števila por, ki je večja pri polkontinuirano ulitih ingotih **(Slika 13 (b)).** To večje število por je najverjetneje posledica večje nagnjenosti k nastanku poroznosti zaradi krčenja v tradicionalnih vzorcih RPT. V naši prejšnji študiji [54] smo ugotovili, da se je po večkratni obdelavi z rotacijskim razplinjevanjem (s čistilnim plinom Ar) v tradicionalnem vzorcu RPT zaradi nizke vsebnosti vodika in bifilma oblikovala velika osrednja krčilna pora. Vendar se lahko ta osrednja krčilna pora na površini prereza vzorca pojavi kot več majhnih por. V tem primeru, zlasti pri 3. polkontinuirano ulitem vzorcu RPT, je situacija podobna: obstaja osrednja krčilna pora, ki se na prečnem prerezu pojavi v obliki ločenih por, kar poveča gostoto števila por.

Rezultati NBI, A_f in NTPP se dobro ujemajo z rezultati pretaljenih vzorcev, pri čemer je očitno, da ima horizontalno

be explained by the deviation of the pores from the spherical shape. No relationship was found between pore number density and pore area fraction **(Figure 10. (f)).** Note that in theory, each relationship is presented in **Figure 10.** should intercept the axis of ordinates at 0. However, to get representative R^2 values, the regression lines were not forced to intercept at 0.

4.4 Traditional RPT samples

The results of the image analysis of traditional RPT samples **(Figure 13)** cast from remelted ingot pieces show a similar difference between DC and gravity cast ingots as in **Table 3**. Almost every investigated parameter is higher for gravity cast ingot samples **(Figure 13 (a))**, which indicates higher bifilm and gas content. The only exception is the pore number density, which is higher in the case of DC cast ingot **(Figure 13 (b)).** This higher number of pores is most probably a result of the higher tendency to shrinkage porosity formation in traditional RPT samples. In our previous study [54], we found that after multiple rotary degassing treatments (with Ar purging gas), a large central shrinkage pore formed in a traditional RPT sample as a result of low hydrogen and bifilm content. However, this central shrinkage pore may appear as several small pores on a sectioned sample surface. In this case, especially for the 3rd DC RPT sample, the situation is similar: there is a central shrinkage pore, which appears as separate pores on the cross-section, which increases pore number density.

NBI, A_f, and NTPP results correlate well with those of the remelted samples, and it is evident that the HDC casting ingot possesses lower oxide and gas concentration. This can be traced back to the differences in the melt preparation and casting technologies. As was highlighted in

polkontinuirano uliti ingot nižjo koncentracijo oksidov in plinov. Razlog za to so razlike v tehnologijah priprave taline in litja. Kot je bilo poudarjeno v uvodu, postopek horizontalnega polkontinuiranega litja ne vključuje litja in taline, ki prosto pada, zato med litjem ne prihaja do nastajanja bifilma. Poleg tega so enote za litje običajno povezane s talilnimi pečmi prek sistema za odstranjevaje nečistoč iz kovin, ki vključuje linije za razplinjevanje in filtrske škatle [16, the introduction, the HDC casting process does not involve any pouring action, and there is no free-falling liquid metal, so there is no bifilm formation during casting. Also, the casting units are generally connected to the melting furnaces through a metal launder system, which involves in-line degassing units and filter boxes [16, 17]. For these reasons, metal cleanliness is often superior to gravity cast ingots, which is supported by our experimental results.

a)				
Parameter	1.	2.	3.	Povprečje / Average
BI [mm]	112,76	132,03	93,01	112,6 ±19,51
NBI [mm/cm^2]	9,21	11,57	8,37	9,72 ±1,66
Af [%]	4,52	5,82	3,01	4,45 ±1,41
Nd [cm^{-2}]	9,31	11,12	10,07	10,17 ±0,91
NTPP [mm/cm^2]	29,50	38,76	26,33	31,53 ±6,46
b)				
Parameter	1.	2.	3.	Povprečje / Average
BI [mm]	103,71	87,85	72,84	88,13 ±15,44
NBI [mm/cm^2]	9,43	7,81	6,69	7,98 ±1,38
Af [%]	2,62	1,57	1,14	1,78 ±0,76
Nd [cm^{-2}]	16,46	15,20	15,07	15,57 ±0,77
NTPP [mm/cm^2]	32,32	25,39	21,88	26,53 ±5,31

Slika 13. Rezultati analize slik kosov RPT, ulitih iz pretaljenih (a) gravitacijsko ulitih in (b) HDC-ulitih vzorcev ingotov

Figure 13. Results of the image analysis of RPT pieces cast from remelted (a) gravity cast and (b) HDC cast ingot samples

17]. Iz teh razlogov je čistost kovine pogosto boljša kot pri gravitacijsko ulitih ingotih, kar potrjujejo tudi naši eksperimentalni rezultati.

4.5 Možni viri napak pri ocenjevanju kakovosti

Tiryakioğlu in drugi [55] so poročali, da v vzorcih RPT obstajajo bifilmi, ki se med strjevanjem ne odprejo in napihnejo v pore. Zato *Olofsson* in drugi [56] navajajo, da je poroznost le vidni (ali lažje zaznavni) del poškodb zaradi zajemanja zraka. To kaže, da RPT običajno podcenjuje količino bifilma. Število neodprtih bifilmov (skritih poškodb zaradi zajemanja zraka) je lahko še posebej veliko, kadar je vsebnost raztopljenega vodika v materialu nizka [57]. Na podlagi tega bi lahko v vzorcih obstajali neodprti bifilmi, ki jih med našim pregledom nismo zaznali, kar pomeni, da so količinsko opredeljeni le tisti bifilmi, ki lahko med strjevanjem tvorijo pore. Ta negotovost trenutno velja za večino (če ne za vse) metod ocenjevanja kakovosti taline, ki temeljijo na preskusih z zmanjšanim tlakom. Vendar pa je treba poudariti, da so se pore v ponovno taljenih vzorcih v primerjavi s tradicionalnimi vzorci RPT povečale, kar je neposredno razvidno iz višjih vrednosti deleža površine por v ponovno taljenih vzorcih **(Preglednica 3 in Slika 13).** Razlog za to je mogoče iskati v tem, da so ponovno taljeni vzorci sprva dlje časa v tekočem stanju **(Slika 9),** kar omogoča popolnejše napihovanje bifilma. S tega vidika pretaljeni vzorci zagotavljajo natančnejše informacije o vsebnosti bifilma kot tradicionalni vzorci RPT.

Ker so pretaljeni vzorci razmeroma majhni, se pojavi sum, da lahko talina absorbira vodik iz atmosfere v peči ali pa izgublja vodik zaradi naravnega razplinjevanja [58]. Prva možnost je bila preizkušena s pretaljenjem vzorca,

4.5 Possible sources of error in quality evaluation

Tiryakioğlu et al. [55] reported that there are bifilms in RPT samples that fail to open up and inflate into pores during solidification. For this reason, it is stated by *Olofsson* et al. [56] that porosity is only the visible (or the more easily detectable) part of the entrainment damage. This indicates that RPT tends to underestimate the bifilm quantity. The number of unopened bifilms (hidden entrainment damage) can be especially high when the solute hydrogen content is low [57]. Based on this, there could be unopened bifilms in the samples that were not detected during our investigation, which means that only those bifilms are quantified that can form pores during solidification. This uncertainty currently applies to most (if not all) melt quality evaluation methods, which rely on reduced-pressure tests. However, it should be highlighted that the pores have grown larger in remelted samples compared to traditional RPT specimens, which can be directly seen in the higher pore area fraction values of remelt samples **(Table 3 and Figure 13)**. The possible reason for this is that initially, the remelted samples stay in the liquid state for a longer time **(Figure 9)**, which allows a more complete bifilm inflation. From this point of view, remelted samples provide more accurate information about the bifilm content than traditional RPT specimens.

As the remelted samples are relatively small, the suspicion arises that the liquid metal may absorb hydrogen from the furnace atmosphere, or it may lose hydrogen due to natural degassing [58]. The former possibility was tested by remelting a sample extracted from a degassed batch that had a density of 2.67 g/cm^3. After remelting and solidifying in a vacuum chamber at 80 mbar, the density

pridobljenega iz razplinjene serije z gostoto 2,67 g/cm^3. Po pretaljevanju in strjevanju v vakuumski komori pri tlaku 80 mbar je gostota vzorca ostala enaka, kar kaže, da absorpcija vodika v 15 minutah taljenja ni predstavljala težave. Avtorji menijo, da je naravno razplinjevanje zanemarljivo tudi ob upoštevanju, da se med enournim predgrevanjem pri 500 °C in postopkom taljenja na površini vzorca tvori razmeroma debela oksidna plast. Poročali so, da sta stopnji absorpcije in desorpcije vodika skozi neporušeno oksidno plast tekočega Al pri temperaturah pod 800 °C približno 1–3 ml·m^{-2}·h^{-1}. Ta hitrost reakcije se z nenehnim motenjem površine taline poveča na 10^4 ali 10^5 ml·m^{-2}·h^{-1} [59]. V preučevanem primeru je praktični pomen tega ta, da lahko zanemarimo prenos vodika med vzorcem in atmosfero v peči, razen če je oksidna plast na površini taline motena. Pri tradicionalnih vzorcih RPT se zdi, da je sčasoma do določene mere prišlo do naravnega razplinjevanja, saj je bil delež površine por bistveno manjši pri tretjih vzorcih RPT, ki so bili uliti približno 15 minut po odvzemu prvih vzorcev **(Slika 13).** S tega vidika je mogoče s pretaljenimi vzorci dobiti natančnejše rezultate.

Prav tako je treba omeniti, da pri preiskavah pretaljevanja niso bili upoštevani deli z luknjami zaradi krčenja na osrednjem delu ingota **(Slika 4 (d)).** Če so povezani s površino (ali jih sproži bifilm), imajo ti deli že oksidirano površino, kar poveča oksidacijsko obremenitev serij, izdelanih s taljenjem teh ingotov. Ta metoda preiskave tega očitno ne odraža.

5 Zaključek

Na podlagi eksperimentalnih rezultatov, podrobno opisanih v tej študiji, je mogoče oblikovati naslednje sklepe:

of the sample remained the same, which indicates that hydrogen absorption was not an issue during the 15 minutes of the melting procedure. It is the authors' opinion that natural degassing is also negligible, taking into account that a relatively thick oxide layer forms on the sample surface during the 1-hour-long preheating at 500 °C and the melting procedure. It was reported that the absorption and desorption rates of hydrogen through an undisturbed oxide layer of liquid Al at temperatures below 800 °C are about 1–3 ml·m^{-2}·h^{-1}. This reaction rate is increased to 10^4 or 10^5 ml·m^{-2}·h^{-1} by the continuous disturbance of the melt surface [59]. In the examined case, the practical meaning of this is that unless the oxide layer on the melt surface is disturbed, hydrogen transport between the sample and the furnace atmosphere can be neglected. By taking traditional RPT specimens, it appears that with time, natural degassing occurred to some degree as the pore area fraction was significantly less in the case of the 3rd RPT samples, which were cast approximately 15 minutes after taking the 1st samples **(Figure 13)**. From this point of view, remelted samples provide more accurate results.

It is also worth noting that for the remelting investigations, the parts with shrinkage cavities in the central region of the ingot were not considered **(Figure 4 (d))**. These, if they are connected to the surface (or initiated by a bifilm) already have an oxidized surface, which increases the oxide load of the batches made by melting these ingots. This is clearly not reflected by this investigation method.

5 Conclusion

Based on the experimental results detailed in this study, the following conclusions can be drawn:

- Metodo vrednotenja kakovosti, ki sta jo predlagala *Fox* in *Campbell* [19], je mogoče uspešno uporabiti za določanje vsebnosti bifilma in plina (vodika in zajetega zraka) v trdnih materialih ingota. Metodo je mogoče uporabiti za ocenjevanje kakovosti vseh vrst trdnih vzorcev, kot so deli ulitih delov ali tekočih sistemov.
- Simulacije strjevanja, termična analiza in mikrostrukturne preiskave so pokazale, da so z uporabo predlagane geometrije vzorca in tehnike pretaljevanja razlike v pogojih strjevanja tradicionalnih in pretaljenih vzorcev RPT premajhne, da bi jih lahko odkrili z mikrostrukturnimi preiskavami.
- Horizontalno polkontinuirano uliti ingoti imajo nižje koncentracije bifilma in plina, kar je mogoče pripisati razlikam v tehnologijah ulivanja ingotov: gravitacijsko uliti ingoti se vlivajo turbulentno, kar povzroča močnejši zajem zraka in oksidnega filma. K slabši kakovosti kovine prispevajo tudi luknje zaradi krčenja v gravitacijsko ulitih ingotih.
- Obstaja močna linearna korelacija med normaliziranimi vrednostmi indeksa bifilma in skupnim obsegom por, kar kaže, da se indeks bifilma lahko uporablja za napovedovanje skupne površine por.

Zahvala

Podprto s strani ÚNKP-22-3 Nov nacionalni program za odličnost Ministrstva za kulturo in inovacije iz vira Nacionalnega sklada za raziskave, razvoj in inovacije. Avtorji se zahvaljujejo družbi NovaCast Systems AB za podporo.

- The quality evaluation method proposed by *Fox* and *Campbell* [19] can be successfully applied for the characterization of the bifilm and gas (hydrogen and entrained air) content of solid ingot materials. The method holds the potential to be applicable for the quality evaluation of any type of solid samples, such as sections of cast parts or running systems.
- Solidification simulations, thermal analysis, and microstructural investigations revealed that by using the proposed sample geometry and remelting technique, the differences in the solidification conditions of traditional and remelt RPT samples are too small to be uncovered by microstructural investigations.
- HDC cast ingots possess lower bifilm and gas concentrations, which can be traced back to the differences in the casting technologies of the ingots: gravity cast ingots are poured turbulently, which results in more severe air and oxide film entrainment. Shrinkage cavities in gravity cast ingots also contribute to lower metal quality.
- There is a strong linear correlation between the normalized values of Bifilm-Index and the total pore perimeter, which indicates that Bifilm-Index can be used for the prediction of total pore surface area.

Acknowledgment

Supported by the ÚNKP-22-3 New National Excellence Program of the Ministry for Culture and Innovation from the source of the National Research, Development and Innovation Fund. The authors thank the support of NovaCast Systems AB.

References

1. J. Campbell, Complete Casting Handbook, 2nd edn. (Elsevier Ltd. 2015) http://dx.doi.org/10.1016/B978-0-444-63509-9.00002-9
2. J. Campbell, The Mechanisms of Metallurgical Failure - The Origin of Fracture. (Elsevier Ltd. 2020) https://doi.org/10.1016/B978-0-12-822411-3.00001-0
3. J. Campbell, A Personal View of Microstructure and Properties of Al Alloys. Materials, 14, 1297 (2021) https://doi.org/10.3390/ma14051297
4. J. Campbell, Castings Practice - The 10 Rules of Castings, (Elsevier Ltd. 2004) pp. 2-8
5. M. Jolly, Prof. John Campbell's Ten Rules for Making Reliable Castings. JOM 57, 19–28 (2005) https://doi.org/10.1007/s11837-005-0091-4
6. E. Erzi, Ö. Gürsoy, C. Yüksel, et al. Determination of Acceptable Quality Limit for Casting of A356 Aluminium Alloy: Supplier's Quality Index (SQI). Metals, 9, 957 (2019) https://doi.org/10.3390/met9090957
7. https://www.foundrymag.com/melt-pour/media-gallery/21258063/reducing-foundry-scrap-starts-with-melt-control-porosity-solutions-inc
8. J. Campbell, "Stop Pouring, Start Casting". Inter Metalcast 6, 7–18 (2012) https://doi.org/10.1007/BF03355529
9. J. F. Grandfield, Remelt Ingot Production Technology. in Essential Readings in Light Metals, ed. by J. F. Grandfield, D. G. Eskin (Springer, 2016), pp. 1003–1010 https://doi.org/10.1007/978-3-319-48228-6_127
10. V. Nguyen, P. Rohan, J. Grandfield, et al. Implementation of CASTfill Low-Dross Pouring System for Ingot Casting. Mater Sci Forum 693, 227–234 (2011) https://doi.org/10.4028/www.scientific.net/MSF.693.227
11. M. Prakash, P. Cleary, J. Grandfield, Modelling of Metal Flow and Oxidation during Furnace Emptying Using Smoothed Particle Hydrodynamics. J Mater Process Technol 209, 3396–3407 (2009) https://doi.org/10.1016/j.jmatprotec.2008.07.055
12. M. Prakash, P. Cleary, J. Grandfield, et al. Optimisation of Ingot Casting Wheel Design Using SPH Simulations. Prog Comput Fluid Dyn 7, 101–110 (2007) https://doi.org/10.1504/pcfd.2007.013002
13. J. F. Grandfield, The Problem of Cavities in Open Mold Conveyor Remelt Ingots. in Light Metals 2016, ed. by E. Williams (Springer 2016) pp. 797-801https://doi.org/10.1002/9781119274780.ch135
14. D. V. Neff, Metal Melting & Handling, (NADCA, 2018) pp. 10-12
15. J. F. Grandfield, D. G. Eskin, I. F. Bainbridge, Direct-Chill Casting of Light Alloys: Science and Technology, (TMS, 2013) pp. 273-279
16. F. Niedermair, H. Zeillinger, Horizontal Direct Chill (HDC) Casting of Aluminium - the HE Universal Caster. in Continuous Casting: Proceedings of the International Conference on Continuous Casting of Non-Ferrous Metals, (2006) pp. 336–343
17. F. Niedermair, Horizontal Direct Chilled (HDC) Casting Technology for Aluminium and Requirements to Metal Cleanliness. Proc. Aust. Asian Pacific Conf. Alum. Cast House Technol. (2001) pp. 253–262
18. S. Fox, J. Campbell, Visualisation of Oxide Film Defects During Solidification of Aluminium Alloys. Scr Mater 43, 881–886 (2000) https://doi.org/10.1016/S1359-6462(00)00506-6

19. S. Fox, J. Campbell, Liquid Metal Quality. Int J Cast Met Res 14, 335–340 (2002) https://doi.org/10.1080/13640461.2002.11819451
20. D. Dispinar, J. Campbell, Critical Assessment of Reduced Pressure Test. Part 1: Porosity Phenomena. Int J Cast Met Res 17, 280–286 (2004) https://doi.org/10.1179/136404604225020704
21. R. DasGupta, Approaches to Measurement of Metal Quality. in ASM Handbook Volume 15, Casting, (ASM International, 2008) pp. 1167–1173 https://doi.org/10.31399/asm.hb.v15.a0005340
22. D. Dispinar, J. Campbell, Use of Bifilm Index as an Assessment of Liquid Metal Quality. Int J Cast Met Res 19, 5–17 (2006) https://doi.org/10.1179/136404606225023300
23. D. Dispinar, J. Campbell, Effect of Casting Conditions on Aluminium Metal Quality. J Mater Process 182, 405–410 (2007) https://doi.org/10.1016/j.jmatprotec.2006.08.021
24. E. Erzi, M. Tiryakioğlu, A Simple Procedure to Determine Incoming Quality of Aluminum Alloy Ingots and Its Application to A356 Alloy Ingots. Inter Metalcast 14, 999–1004 (2020) https://doi.org/10.1007/s40962-020-00414-5
25. F. Y. Hsu, C. L. Li, Runner Systems Containing Ceramic Foam Filters Quantified by “Area Normalized” Bifilm Index Map. Inter Metalcast 9, 23–35 (2015) https://doi.org/10.1007/BF03355620
26. G. Sigworth, Understanding Quality in Aluminum Castings. Inter Metalcast 5, 7–22 (2011) https://doi.org/10.1007/BF03355504
27. A. M. Samuel, F. H. Samuel, H. W. Doty, S. Valtierra, Porosity Formation in Al-Si Sand Mold Castings. Inter Metalcast 11, 812–822 (2017) https://doi.org/10.1007/s40962-016-0129-0
28. S. Akhtar, L. Arnberg, M. Di Sabatino, et al. A Comparative Study of Porosity and Pore Morphology in a Directionally Solidified A356 Alloy. Inter Metalcast 3, 39–50 (2009) https://doi.org/10.1007/BF03355440
29. M. H. Mulazimoglu, N. Handiak, J. E. Gruzleski, Some Observations on the Reduced Pressure Test and Hydrogen Concentration of Modified A356 Alloy. AFS Trans 97, 225–232 (1989)
30. N. Zhang, X. Yu, A. Pradhan, A. J. Puppala, Effects of Particle Size and Fines Content on Thermal Conductivity of Quartz Sands. Transp. Res. Rec., 2510(1), 36–43 (2015) https://doi.org/10.3141/2510-05
31. G. Gyarmati, Gy. Fegyverneki, M. Tokár, T. Mende, Effect of the Sampling Method on the Results of Melt Quality Assessment of Aluminum Alloys with Computed Tomography. IOP Conf Ser Mater Sci Eng 903, 012003 (2020) https://doi.org/10.1088/1757-899X/903/1/012003
32. G. Gyarmat, Gy. Fegyverneki, T. Mende, M. Tokár, Characterization of the Double Oxide Film Content of Liquid Aluminum Alloys by Computed Tomography. Mater Charact 157, 109925 (2019) https://doi.org/10.1016/j.matchar.2019.109925
33. D. Dispinar, J. Campbell, Critical Assessment of Reduced Pressure Test. Part 2: Quantification. Int J Cast Met Res 17, 287–294 (2004) https://doi.org/10.1179/136404604225020704
34. G. K. Sigworth, Fundamentals of Solidification in Aluminum Castings. Inter Metalcast 8, 7–20 (2014) https://doi.org/10.1007/BF03355567

35. M. C. Flemings, T. Z. Kattamis, B. P. Bardes, Dendrite Arm Spacing in Aluminum Alloys. AFS Trans 99, 501–506 (1991)
36. V. Rontó, A. Roósz, The Effect of Cooling Rate and Composition on the Secondary Dendrite Arm Spacing during Solidification. Part I: Al-Cu-Si Alloys. Int J Cast Met Res 13, 337–342 (2001) https://doi.org/10.1080/13640461.2001.11819415
37. M. D. Peres, C. A. Siqueira, A. Garcia, Macrostructural and Microstructural Development in Al-Si Alloys Directionally Solidified Under Unsteady-State Conditions. J Alloys Compd 381, 168–181 (2004) https://doi.org/10.1016/j.jallcom.2004.03.107
38. U. Feurer, R. Wunderlin, in W. Kurz, D. J. Fisher (Eds.), Fundamentals of Solidification, (Trans Tech Publications Ltd., 1992) pp. 85-86
39. D. H. Kirkwood, A Simple Model for Dendrite Arm Coarsening during Solidification. Mater Sci Eng 73, L1 (1985) https://doi.org/10.1016/0025-5416(85)90319-2
40. G. Kaptay, E. Báder, L. Bolyán, Interfacial Forces and Energies Relevant to Production of Metal Matrix Composites. Mater Sci Forum 329, 151–156 (2000) https://doi.org/10.4028/www.scientific.net/msf.329-330.151
41. A. L. Greer, A. M. Bunn, A. Tronche, et al. Modelling of Inoculation of Metallic Melts: Application to Grain Refinement of Aluminium by Al-Ti-B. Acta Mater 48, 2823–2835 (2000) https://doi.org/10.1016/S1359-6454(00)00094-X
42. Y. Du, Y. A. Chang, B. Huang, et al. Diffusion Coefficients of Some Solutes in FCC and Liquid Al: Critical Evaluation and Correlation. Mater Sci Eng A 363, 140–151 (2003) https://doi.org/10.1016/S0921-5093(03)00624-5
43. M. Uludağ, R. Çetin, D. Dişpinar, M. Tiryakioğlu, On the Interpretation of Melt Quality Assessment of A356 Aluminum Alloy by the Reduced Pressure Test: The Bifilm Index and Its Physical Meaning. Inter Metalcast 12, 853–860 (2018) https://doi.org/10.1007/s40962-018-0217-4
44. D. Dispinar, J. Campbell, Porosity, Hydrogen and Bifilm Content in Al Alloy Castings. Mater Sci Eng A 528, 3860–3865 (2011) https://doi.org/10.1016/j.msea.2011.01.084
45. D. Dispinar, A. Kvithyld, A. Nordmark, Quality Assessment of Recycled Aluminium. in Light Metals 2011, ed. by S. J. Lindsay (Springer, 2011) pp. 731–735 https://doi.org/10.1002/9781118061992.ch127
46. M. Uludağ, R. Çetin, L. Gemi, D. Dispinar, Change in Porosity of A356 by Holding Time and Its Effect on Mechanical Properties. J Mater Eng Perform 27, 5141–5151 (2018) https://doi.org/10.1007/s11665-018-3534-0
47. C. Yuksel, O. Tamer, E. Erzi, et al. Quality Evaluation of Remelted A356 Scraps. Arch Foundry Eng 16, 151–156 (2016) https://doi.org/10.1515/afe-2016-0069
48. D. Dispinar, Melt Quality Assessment. in Encyclopedia of Aluminum and Its Alloys, ed. by G. E. Totten, M. Tiryakioğlu, O. Kessler (Taylor & Francis, 2019) pp. 1430–1445 https://doi.org/10.1201/9781351045636-120052503
49. D. Dispinar, J. Campbell, A Comparison of Methods Used to Assess Aluminium Melt Quality. in: Shape Casting 2nd International Symposium, ed. by P. N. Crepeau, M. Tiryakioglu, J. Campbell, (TMS, 2007) pp. 11–18
50. M. Uludağ, R. Çetin, D. Dispinar, M. Tiryakioğlu, The Effects of Degassing, Grain Refinement & Sr-addition on Melt Quality-Hot Tear Sensitivity Relationships in Cast A380 Aluminum Alloy. Eng Fail Anal 90, 90–102 (2018) https://doi.org/10.1016/j.engfailanal.2018.03.025

51. W. LaOrchan, M. H. Mulazimoglu, J. E. Gruzleski, Quantification of Reduced Pressure Test. AFS Trans 99, 653–659 (1991)
52. D. Dispinar, J. Campbell, Reduced Pressure Test (RPT) for Bifilm Assessment. in Shape Casting: 5th International Symposium, ed. by M. Tiryakioglu, J. Campbell, G. Byczynski (TMS, 2014) pp. 243–251 https://doi.org/10.1007/978-3-319-48130-2_30
53. H. Song, L. Zhang, F. Cao, et al. Three-Dimensional Reconstruction of Bifilm Defects. Scr Mater 191, 179–184 (2020) https://doi.org/10.1016/j.scriptamat.2020.09.040
54. G. Gyarmati, F. Vincze, Gy. Fegyverneki, et al. The Effect of Rotary Degassing Treatments with Different Purging Gases on the Double Oxide- and Nitride Film Content of Liquid Aluminum Alloys. Metall Mater Trans B 53, 1244–1257 (2022) https://doi.org/10.1007/s11663-021-02414-0
55. M. Tiryakioğlu, P. Yousefian, P. D. Eason, Quantification of Entrainment Damage in A356 Aluminum Alloy Castings. Metall Mater Trans A 49, 5815–5822 (2018) https://doi.org/10.1007/s11661-018-4865-z
56. J. Olofsson, T. Bogdanoff, M. Tiryakioglu, Revealing and Simulating the Effect of Hidden Damage on Local and Full-Field Deformation Behaviour of Cast Aluminium. IOP Conf Ser Mater Sci Eng 1281, 012066 (2023) https://doi.org/10.1088/1757-899X/1281/1/012066
57. M. Riestra, A. Bjurenstedt, T. Bogdanoff, et al. Complexities in the Assessment of Melt Quality. Inter Metalcast 12, 441–448 (2018) https://doi.org/10.1007/s40962-017-0179-y
58. M. Syvertsen, A. Kvithyld, E. Gundersen, et al. Furnace Atmosphere and Dissolved Hydrogen in Aluminium. in Light Metals 2019, ed by C. Chesonis (TMS, 2019) pp. 1051–1056 https://doi.org/10.1007/978-3-030-05864-7_128
59. J. Weigel, E. Fromm, Determination of Hydrogen Absorption and Desorption Processes in Aluminum Melts by Continuous Hydrogen Activity Measurements. Metall Mater Trans B 21, 855–860 (1990) https://doi.org/10.1007/BF02657810